Journal of African Earth Sciences 235 (2026) 105964

Contents lists available at ScienceDirect

Journal of African Earth Sciences

journal homepage: www.elsevier.com/locate/jafrearsci

Unconformity-related fluorite-baryte-base metal mineralization in the Benue Trough, Nigeria: A multifluid origin triggered by the separation of Pangaea

Benjamin F. Walter [a,b,c,*], Ndukauba Egesi [d], Mohsin Raza [b,c,e], Micheal Agbebia [d], Fadila Adamu [b,c], R. Johannes Giebel [f,g], Michael A.W. Marks [a], Emmanuel Chidi Ugbaja [d], Gregor Markl [a]

[a] Petrology and Mineral Resources, Department of Geoscience, University of Tübingen, Schnarrenbergstrasse 92-94, Tübingen, Germany
[b] Chair of Economic Geology and Geochemistry (EGG), Institute of Applied Geosciences (AGW), Karlsruhe Institute of Technology (KIT), Adenauerring 20b, 76131, Karlsruhe, Germany
[c] Laboratory for Environmental and Raw Material Analyses (LERA), Institute of Applied Geosciences (AGW), Karlsruhe Institute of Technology (KIT), Adenauerring 20b, 76131, Karlsruhe, Germany
[d] Department of Geology, University of Port Harcourt, Port Harcourt, Nigeria
[e] Department of Geology, Bacha Khan University Charsadda, Charsadda, Khyber Pakhtunkhwa Pakistan
[f] Technische Universität Berlin, Institute of Applied Geosciences, Ernst-Reuter-Platz 1, 10587, Berlin, Germany
[g] University of the Free State, Department of Geology, 250 Nelson-Mandela-Drive, 9300, Bloemfontein, Republic of South Africa

ARTICLE INFO

Handling Editor: M Mapeo

ABSTRACT

Unconformity-related hydrothermal vein-type deposits are key sources of high-purity fluorite, baryte, and base metals, with occurrences in Nigeria, particularly along the Benue Trough. However, the genesis of the Nigerian deposits is not well understood. This study examines fluid inclusion systematics from mineralized veins at Enyigba, Ameta, Ikwo, Otim Land, and Uburu-Abakaliki, using microthermometry, crush-leach analysis, and Raman spectroscopy. Fluid inclusion microthermometry reveals homogenization temperatures between 99 and 190 °C and salinities of 18.3–22 wt%NaCl + $CaCl_2$, typical of unconformity-related hydrothermal vein systems. Geochemical data indicate the mineralizing fluids resulted from mixing of bittern brines (low Cl/Br), halite-dissolution brines (high Cl/Br), and oilfield brines, as shown by Cl/Br ratios and Rb/Cs values. Microraman spectroscopy suggests the presence of hydrocarbons, supporting the involvement of reduced oilfield brines. These findings point to a complex fluid mixing process, likely driven by crustal-scale faulting during the rifting of the Benue Trough in the context of Pangaea break-up. This research suggests a common ore-forming process for the Nigerian deposits.

1. Introduction

Acid grade, high-purity fluorite and baryte are essential basic compounds for the chemical industry applications and classified by the European Commission (European Commission, 2020) as critical raw material (CRMs). Worldwide, about 7.6 million tons and about 8 million tons, respectively, fluorite and baryte is produced. China (62 %), Mexico (12 %) and Mongolia (12 %) are the three largest producers (Nassar et al., 2025).

Unconformity-related hydrothermal fluorite-baryte vein type deposits are usually hosted in upper crustal and brittle tectonic settings, and typically contain a diverse base metal mineralization including commodities like Pb, Ag, Zn, Cu, Bi and Sb. They can be observed below or above a lithological unconformity separating sedimentary non-metamorphose rocks from underlain crystalline or metamorphic basement rocks (e.g. Boiron et al., 2010; Burisch et al., 2022; Dill et al., 1986; 1988a, 2012 Walter et al., 2024). Such veins are often a few cm to dm in thickness but can also reach several meters, with the Käfersteige vein in northern Schwarzwald (Germany) being an exemplary vein with up to 30m thickness (Staude et al., 2009 and references therein). The ore body architecture is typically vertical and often show pinch and swallow structures. Such hydrothermal vein type deposits hosting significant

* Corresponding author. Petrology and Mineral Resources, Department of Geoscience, University of Tübingen, Schnarrenbergstrasse 92-94, Tübingen, Germany.
E-mail address: b.walter@uni-tuebingen.de (B.F. Walter).

https://doi.org/10.1016/j.jafrearsci.2025.105964
Received 25 September 2025; Received in revised form 2 December 2025; Accepted 4 December 2025
Available online 5 December 2025

amounts of high purity fluorite and baryte and are very abundant in northern America, Europe and Africa mainly along the Atlantic Ocean coasts (Banks et al., 2002; Boiron et al., 2010; Dill and Weber, 2010; Burisch et al., 2022; Carignan et al., 1997; Cherai et al., 2023; Crognier et al., 2018; Deane, 1995; Grandia et al., 2000; Leach et al., 2004; Subías and Nieto, 1995; Rddad et al., 2022, 2023, 2024, 2025; Richard et al., 2016).

It is widely accepted that fluid mixing between hot (~350 °C), deep-seated (up to 16 km) F- and Ba-enriched basinal or basement brines and chemically contrasting much colder (~50 °C), shallow (<5 km), Ca-and SO_4-enriched connate fluids (that partly interacted with halite formations) from sedimentary rock sequences (typically forming the overburden) is the major ore forming process (e.g. Hoeve and Sibbald, 1978; Carignan et al., 1997; McCaig et al., 2000; Wilkinson, 2010; Fusswinkel et al., 2013, 2014; Bons et al., 2014; Walter et al., 2019, 2017; Richard et al., 2016; Burisch et al., 2022). Fluid cooling is only recognized as a late stage phenomenon and is not sufficient to precipitate significant amounts of fluorite and baryte because of the low solubility products of CaF_2 and $BaSO_4$ which suppress the transportation of fluorine, calcium, barium and sulfate together in the same fluid (Nordstrom and Jenne, 1977; Henry, 2018 and references therein).

Only a limited number of contributions deal with the provenance of the base metals, barium and fluorine in the hydrothermal system. The available literature clearly implies that primary minerals of the crystalline or metamorphic basement are the major base metal host. The same studies provide strong evidence that the base metals are released into the ore fluid during intense million years long-term hydrothermal alteration of sheet-silicates and feldspars in the presence of a high salinity brine with salinities between 20 and 30 wt% NaCl + $CaCl_2$ (Burisch et al., 2016a; Walter et al., 2019; Fusswinkel et al., 2013, 2014; Boiron et al., 2010, Kluge et al., 2024, Jungmann et al., 2025). The high salinity of such a deep-seated brine is essential as the base metals are transported under upper crustal conditions dominantly as chlorine-complexes. In the last decade, fluid flow models for upper crustal conditions fluid mixing processes were significantly refined by the introduction of a two-component or multi-component "fluid mixing from below" model which combines hydrological fluid and rock properties with geochemical data sets (e.g. Bons et al., 2014; Walter et al., 2019). To develop ore-forming upper crustal mixing processes, a fluid separation into significantly geochemically contrasting aquifers in the basement and sedimentary rocks is required (Bons et al., 2014; Walter et al., 2017, 2018a,b) and therefore the development of a "fluid unconformity" even within a single rock unit is an essential prerequisite (Burisch et al., 2022)

Since most crustal fluids are oxidized, it is easy to explain the formation of baryte and carbonates. However reduced conditions are required to enable the transport of sulfide anions or to reduce sulfate in the metal carrier fluid to develop base metal mineralization (Markl et al., 2016; Burisch et al., 2017a, Kreissl et al., 2018; Walter et al., 2019; Scharrer et al., 2019, 2021, 2022). Therefore it was a major challenge of the last decade to decipher the reasons for the observations of barren veins that can occur next to veins hosting significant base metal mineralization like Zn, Pb, Ag, Sb, Cu (and sometimes in ore shoots Ni and Co, Scharrer et al., 2022). One key aspect is likely the absence or presents of CH_4 and H_2S as reducing agents at the time of fluid mixing which is therefore a key prerequisite suppressing or allowing base metal ore precipitation (Burisch et al., 2017a; Scharrer et al., 2019, 2021).

In Africa, unconformity-related hydrothermal vein type deposits (partly including base metal mineralization) are widespread in Morocco (Rddad et al., 2023, 2024, 2025) and on the west coast of Africa in particular Namibia (Hoal, 1992; Walter et al., 2024). Numerous unstudied locations are, furthermore, identified in the Northern Cape Province in the Republic of South Africa (Walter et al., 2023, 2024 and references therein) and along the Benue Trough in Nigeria (Oha et al., 2017Andrew-Oha et al., 2017; Ogundipe et al., 2017; Emmanuel et al., 2020). The Nigerian deposits along the Benue Trough have been studied to some detail but a holistic model explaining the huge amount of unconformity-related hydrothermal vein type deposits in the failed arm of the rift is still pending (Olade and Morton, 1985; Akande et al., 1989; Akande and Mucke, 1989; Akande and Mücke, 1993; Tijani, 2004; Ene et al., 2012; Obiora et al., 2016; Labe et al., 2018a, b; Oha et al., 2017Andrew-Oha et al., 2017, Ogundipe et al., 2017; Emmanuel et al., 2020). Since not much scientific attention has been spend on the Nigerian deposits, understanding the properties of the ore formation in the fluorite-baryte mineral system is crucial to develop new exploration vectors to target the important industrial mineral occurrences of fluorite and baryte in underexplored areas like Nigeria. This contribution addresses the Enyigba, Ameta and Uburu-Abakakili Area Lead-Zinc deposits and Otimland Obubura area in southeastern Nigeria and focuses on the following aspects.

- a study deciphering the ore-forming fluids by application of microthermometry and crush leach analysis of various samples from five Nigerian deposits;
- development of a genetic model for fluorite-baryte precipitation in southeastern Nigeria in the context of the close-by rift triple junction during onset of Gondwana break up.

1.1. Geology of Nigeria

The Precambrian basement of Nigeria is distinguished into the following five units (Obaje, 2009 and references therein): (I) The Migmatite–Gneiss Complex (MGC) which contains amphibolite-facies granite-gneisses and highly metamorphic migmatites, with minor amphibolites, quartzites and metasedimentary rocks. (II) The NNE-SSW oriented Nigeria Schist Belts (metasedimentary and metavolcanic rocks) is mainly composed of greenschist to amphibolite facies metasedimentary rocks (quartzites, marbles, biotite schists, phyllites and amphibolites). The units (I) and (II) are followed by The Older Granite unit (III) which comprises syn-to late-tectonic Pan-African granitoids of granitic-granodioritic composition (with minor syenites, monzonites, gabbros and charnockites) that intrude units I and II, and therefore clearly provide an age relationship. (IV) Later and undeformed muscovite-, tourmaline- and beryl-bearing pegmatites, aplites and syenites, basalts, and lamprophyres intrude and cross cut units I-III. The Mesozoic Younger Granites and Volcanic rock unit (V) contains shallow intrusive and volcanic alkaline rocks with characteristic ring structures (Obaje, 2009 and references therein).

Sedimentary rocks which are unconformably deposited on the basement units record onset of sedimentation from Lower Cretaceous (~120 Ma) discontinuously to recent times (Obaje, 2009 and references therein). Older sedimentary rock units are not preserved, due to strong uplift from Paleozoic to early Mesozoic times which lead to exhumation and erosion. The sedimentary rocks are divided into two main cycles (Fig. 1C): Cretaceous to Cenozoic Sedimentary Units (Cycle 1) and Quaternary to recent alluvial deposits (Cycle 2; Obaje, 2009 and references therein).

1.2. Geology of the Benue Trough

The NE-SW-striking Benue Trough failed rift arm is about 800 km long and up to 100–150 km wide and linked to the break-up of Gondwana and the opening of the South Atlantic Ocean during Early Cretaceous (Fig. 1; Obaje, 2009 and references therein). The Early Cretaceous rifting was dominated by terrestrial deposition with very minor fluviatile and lacustrine sequences. Following this first rifting phase, the sedimentary record is dominated by transgressions and regressions with a first depocenter developed in Albian times (~113 Ma). In the context of depocenter formation, the Asu-River Group was formed comprising mudstones and black shales interbedded with black micritic limestone, siltstone and minor arkoses at the base. With evolution of the basin,

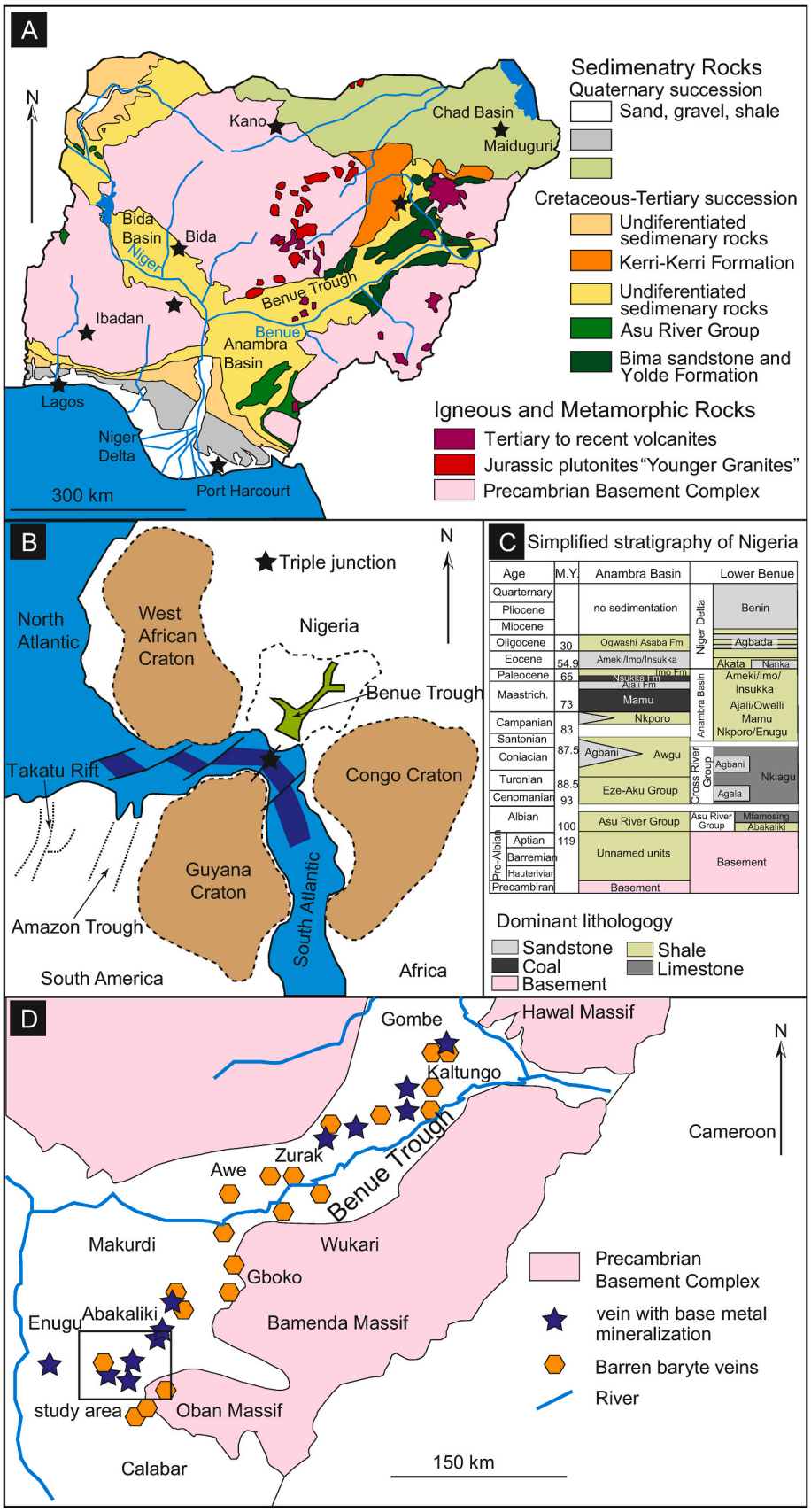

Fig. 1. A) Geological overview map of Nigeria modified after Lar (2013). B) Tectonic position of the Benue Trought after Gubanov and Mooney (2009). C) Distribution of sulfide lodes in the hydrothermal vein system of the Lower Benue Trought. Modified after Ene et al. (2012).

marine limestones and claystones were successively deposited during Maastrichtian including the Upper Cretaceous petroleum system and coal deposits. The sedimentary thickness varies from about 1500m in the southern to over 3000m in the middle Benue Trough (Offodile, 1975; Benkhelil, 1989; Obaje et al., 2004). Basically, the Asu-River Group comprises black shales with intercalations of sandstones, siltstones and limestone (Arinze and Emedo, 2021). The group is further subdivided into three formations which (from bottom to top) are the Mamfe/Awi, Abakaliki and Awe Formations. The rift basin has an asymmetrical architecture with a depth of 2000 m at the northeastern end to over 6000 m in the southwestern region in the vicinity of the Niger Delta. The basin was affected by two phases of tectonic activity (pre-Turonian and Santonian; Obiera et al., 2016). Not much is known about the pre-Turonian event but the Santonian event is characterized by compressional tectonics lead to the development of the NE-SW dominated structures. This phase of tectonic activity is accompanied by uplift of the Abakaliki-Benue fold belt which resulted in a NW-SE and N-S trending extensional fracture network hosting numerous unconformity-related hydrothermal vein type deposits. In the Late Cretaceous, post-deformation subsidence of the basin with extensive coal-forming swamps was the dominant feature of the Benue Trough.

The Benue Trough has still an active geothermal system including ascending brines on structures that partly contain unconformity-related vein-type deposits which are the topic of this contribution. The fluid chemistry is dominated by fluid rock interaction with shales of the Asu-River Group, the Eze-Aku and Agwu Formations (Petters and Ekweozor, 1982; Tijani, 2004). The basinal brines are high salinity Na and Cl fluids with significant components of Ca and Sr. The modern brines of the Benue Trough are strongly depleted in Br, Mg and SO_4 (Tijani, 2004). This leads to high Cl/Br ratios which indicate massive halite dissolution (Laier and Nielsen, 1989). Therefore, the chemical composition of the ascending brine is seen as a result of large-scale fluid mixing between geochemical different fluids or a multiple stepwise evolution of fossil Cretaceous seawater followed by a phase of extensive halite dissolution. The brine evolution also shows a modification through intensive water-rock interactions in basement rocks and the sedimentary rock overburden (albitization of feldspars, dolomitization of limestone and clay mineral formation and interaction; Tijani, 2004).

1.3. The Lower Benue Trough mining district

The Lower Benue Trough is the host of numerous baryte ± fluorite ± base metal vein-type deposits with the areas of the Ishiagu, Enyigba-Ameki-Ameri, Wanikande-Wanakom, and Gabu-Oshina being important mining districts (Akande and Abimbola, 1987, Akande et al. 1989; Oden, 2012, El-Nafaty, 2015, Oha et al., 2017 and references therein) (Fig. 2). The outcrop situation in the tropical environment of Nigeria so far only allows for observations in Albian to Turonian sediments which comprises shale, siltstone, sandstones, providing a likely upper time limit of vein formation <90 Ma (Oha et al., 2017). A notable exception is the Enyigba vein system. On a regional scale the deposits of Enyigba are often spatially associated with older granite intrusions. Close to Wanikande area the baryte veins directly follow the lithological contact between granites and sedimentary rocks (Oha et al., 2017 and references

Fig. 2. Field Photograph of Iyamitet and Okumurutet deposits in Otimland. A) Open pit mining at Iyamitet on a high grade baryte deposits with minor lead-zinc mineralization. B) Granite-hosted quartz-fluorite deposit at Okumurutet. C) Stockpiles at Okumurutet. D) Mineralization of quartz-fluorite veins at Okumurutet. E) Baryt mining site at Okumurutet. F) Disseminated and stratiform baryte mineralization in country rock shales next to the veins at Okumurutet.

therein). The mineralized zones show thicknesses of up to several meters and are up to 2 km long, with only NW-SE and N-S striking veins containing fluorite and/or baryte gangue and partly base metal ores while the dominant NE-SW fractures remain typically sulfide barren (Oha et al., 2017 and references therein). As shown by Oha et al. (2017), Pb:Zn:Ba ratios show an increase in baryte content and a decreasing base metal content towards northeast (3:1:0 at Ishiagu, to 2:1:0 at Enyigba, 1:0:2 at Wanikande and nearly 100 % baryte at Gabu-Oshina). Based on the contribution of Oden (2012), two types of baryte mineralization can be distinguished in Nigeria: (1) the vein-type and (2) stratiform-type deposits within the Benue Trough, whereas vein-type deposits can also be hosted by crystalline basement rocks (Enyigba area). This contribution only focusses on the vein type deposits.

There is a long-lasting debate on the source of Ba which was thought to be related to late magmatic-hydrothermal fluids and, consequently, to igneous activity (Farrington, 1952; Reyment, 1965; Ezepue, 1984; Omada, 1985; Ofoegbu and Odigi, 1989; Omada and Ike, 1996; Tijani et al., 1996; Uma and Loehnert, 1994). Only Orajiaka (1964) discussed variable, potential provenances including both crystalline basement and sedimentary overburden. Already Offodile (1976) proposed juvenile and connate brines together acting as the ore forming fluid. Furthermore, Offodile (1976) already suggested that the sedimentary rock endmember fluid is a halite dissolution brine. This early deposit model was further developed by Olade and Morton (1985) introducing a brine convection model for the Nigerian deposits which is driven by an elevated geothermal gradient typical for failed rift systems like the Benue Trough. A few years later, the Nigerian deposits were again topic of intensive scientific research and the brine convections model of Olade and Morton (1985) was refined into a basinal brine expulsion model by Akande et al. (1989) based on a first set of fluid inclusion and isotope studies on barytes in the Middle and Lower Benue Trough. Today, it is widely accepted that baryte-hosted fluid inclusions do not preserve fluid properties like T_h over geological timescales. Additionally, Akande et al. (1989) explained the brine formation and ascent by sudden dewatering during sedimentary basin overpressurization (“escape bursts“) in the Cretaceous sediment for which however the evidence of typical hydrofracturing breccias is lacking. The leaching of Ba from basement rocks was discussed in the context of mantle plume activity and/or rifting of the Benue Trough (Ofoegbu and Odigi, 1989) but is also outdated based on modern models for brine convection (e.g. Bons et al., 2014).

1.4. The Enyigba, Ameta, Uburu-Abakakili and Otimland Obubura area lead-Zink deposits

In the Lower Benue Trough of Southeastern Nigeria, lead-zinc-barium mineralization manifests as epigenetic, fracture-controlled vein deposits, which are confined to Albian–Turonian sedimentary sequences. Detailed field investigations indicate that mineralization is primarily localized along NW-SE and N-S oriented fractures, whereas the more prevalent NE-SW fractures exhibit no base metal mineralization but baryte and fluorite veins of high purity. All veins (with exception of Enyigba which is basement hosted) are positioned a few meters to hundred meters above the basement-sedimentary cover unconformity.

The Uburu-Abakaliki hydrothermal vein system is the largest and most endowed one within the study area of the Benue Trough and consists of a number of sub-parallel en-echelon mineralized fluorite-baryte-Pb-Zn lodes occurring around the towns of Enyigba, Ameri, Ameka, and Ndiagu (Oha et al., 2017). The Pb-Zn mineralization was discovered and initially explored by the Mineral Survey of Southern Nigeria (Oha et al., 2017). During the operation time 1925–1929, production increased but declined in 1937 due to an economic crisis and related drop of market prices. After a decade with no mining operation, activity increased in the 1950’s under the development of the Nigerian Lead-Zinc Mining Company. Today, exploitation is mainly performed by artisanal miners including indigenous mining companies (Oha et al., 2017). The host rocks of all veins comprise Albian to Coniacian formations (~113-89 Ma) which include the Asu-River Group and the Eze-Aku Group and overly the Lower Cretaceous Abakiliki Shale. The main features associated with the Uburu Abakaliki mineralization are described by Benkhelil (1989) and are summarized below.

Based on the status of modern exploration, the Abakaliki mineralization is likely the most important one in terms of size and density of ore bodies. The Enyigba vein, e. g., has a surface extension of ~ 2 km and a maximum thickness of 30 m. The Ameta vein has a thickness of several meters and a surface exposure of several hundred meters. Based on previous studies, the orebodies contain a sulfide association of galena, sphalerite, siderite, chalcopyrite, pyrite, bornite and quartz. Baryte is widely absent. The hydrothermal mineralization locally contains an early ore stage of diagenetic marcasite, pyrite and minor gel-like colloform-textured schalenblende and galena at the contact to the wall rocks (Akande and Mücke, 1993). The veins also follow NW-SE and N-S trending fractures which are transected in some places by N-S trending sinistral faults of likely post-Jurassic age related to the divergence of America and Africa. The mineralized zones follow the trend of the dominant fracture trend of the Benue Trough.

The Uburu mine which is one of the major targets of this contribution is located in the Umuobuna Uburu, Ohaozara Local Government Area and Onicha Local Government Area of Ebonyi State. The veins strike approximately NW-SE to N-S. Samples gathered at Uburu mine contain mainly baryte veins with galena and minor late-stage quartz. The veins can be traced for several hundred meters with a thickness of several meters.

The Otim Land Area (Obubra veins) hosts the Okumurutet and Iyamitet deposits. The vein set of Okumurutet is dominated by high grade baryte mineralization, but only a minor number of veins show extensive Pb-Zn mineralization. In contrast, the Okumurutet vein set is granite-hosted and contains quartz-fluorite deposits. The general strike direction is NW-SE to N-S. For both vein sets, thicknesses of several meters can be observed. The veins in both sets have a minimum extension of several hundred meters.

The Ikwo vein set is shale-hosted and contains fluorite-baryte-quartz veins with extensive Pb-Zn mineralization. The veins mined at Ikwo are baryte veins with minor amounts of quartz and fluorite. The veins strike roughly N-S and have a thickness of several meters. The veins can be traced in the field for several hundred meters. Not much is known about the deposit, as it is mainly exploited by artisanal mining activities. The Oburu mine is operating on fluorite-baryte-quartz-(±carbonate) veins with galena, sphalerite and tennantite ± chalcopyrite.

2. Sample material

Samples were collected from the Okumurutet mine, Obubra, Otimland (Cross River State), Enyigba and Uburu vein of the Abakaliki district and Ikwo occurrence (Ebonyi State). The mineralization at Uburu mine (Ub1-5), Obubra (OT1-10), Otim Land (OT-B1-4), Enyigba (EN-1-6) and Ikwo (IK1-5) were sampled in 2022 and 2024 (Fig. 3).

3. Analytical methods

3.1. Textural analysis

Transmitted and reflected light microscopy (using Leica Laborlux 12POLS and LEICA DM750P microscopes equipped with Nikon E950 and Olympus E-M5II digital cameras) was done at University of Tübingen on polished thin sections. Microtextures of ore and gangue minerals were studied via carbon-coated samples using a Tabletop Phenom XL scanning electron microscope (SEM) applying back-scattered electron (BSE) imaging with a focused beam and acceleration voltage of 15 kV on low vacuum (10 Pa). Moreover, the elemental mapping on the same thin sections were done by microXRF (Bruker Tornado M4) at the Technische Universität Berlin in the area mode, applying an acceleration voltage of 50 kV and a beam current of 600 μA. Measuring point distance was

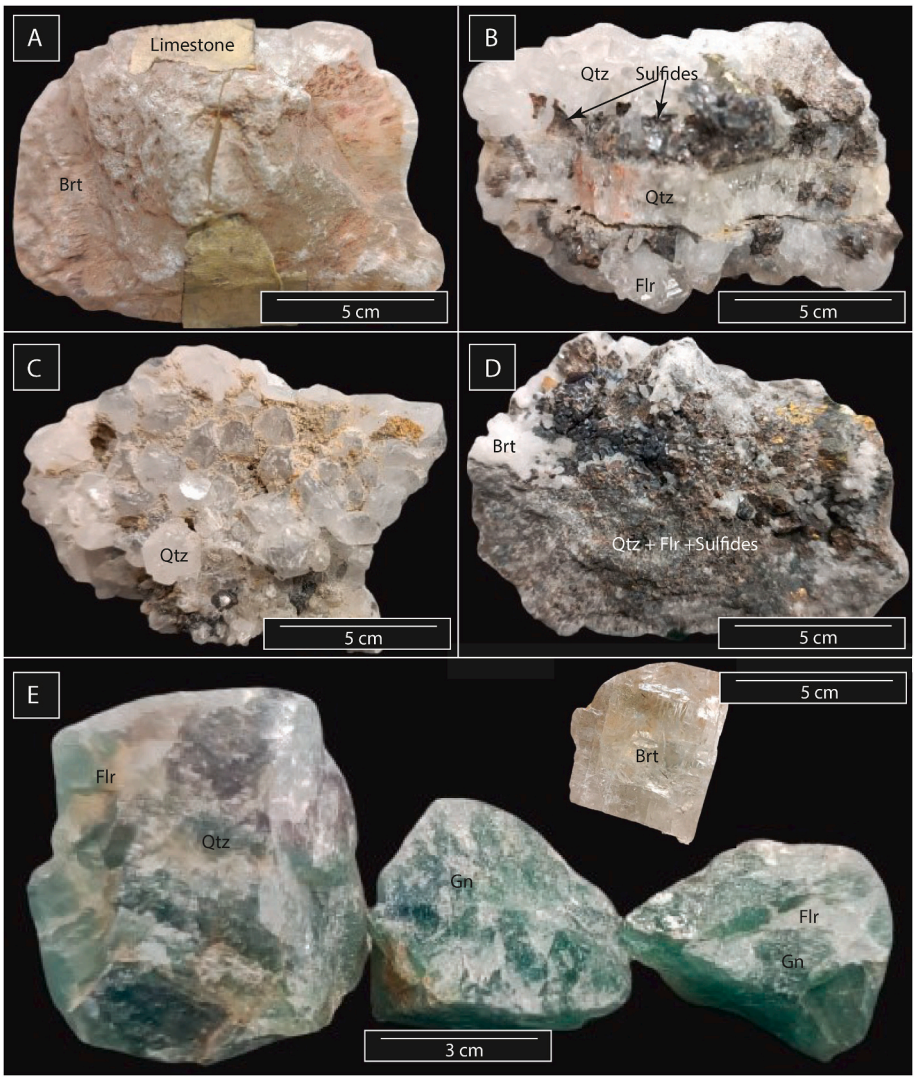

Fig. 3. Representative samples from the locations studied in this contribution. A) Massive baryt mineralization contains clasts of the limestone host rock (Ikwo samples). B) Samples of the Ameta vein set contains sphalerite and galena. C) Euhedral quartz crystals from the Uburo vein set. D) Base metal mineralization at Otim Land occurs prior to baryte. E) Fluorite-quartz samples from the Enyigba vein set.

chosen for 30 μm at 20 μm beam diameter, with a measuring time of 60 ms per spot. For signal improvement, the analyses were done with two simultaneously operating spectrometers.

3.2. Fluid petrography, microthermometry, cathodoluminescence

Eleven representative samples were chosen for microthermometry. Double-polished wafers of 300–400 μm thickness were prepared and studied for their fluid-inclusion inventory and petrography using transmitted light microscopy. The identified fluid inclusions were classified as fluid inclusion assemblages (FIA) following the approach of Goldstein and Reynolds (1994) and are brought into a genetic and temporal relationship as primary (p; hosted by crystal growth zones), pseudo-secondary (ps), secondary (s), isolated (iso) or clustered (c) inclusions (Walter et al., 2015). Each assemblage was checked for potential textural evidence on post entrapment modifications.

After optical investigations to decipher the fluid petrography, the samples were sliced into chips (0.5 × 0.5 cm) for microthermometric analysis. The analyses were done via a Linkam THMS600 heating-freezing device at the Karlsruhe Institute of Technology (KIT). The device was calibrated on a daily basis using synthetic, quartz-hosted H_2O, H_2O-NaCl and H_2O-CO_2 fluid inclusion reference materials (SynFlinc Standard collection) Based on the standard measurements a temperature correction of the measured data was applied. The final cooling temperature of all the inclusions was -190 ^{o}C. To exclude metastable behaviour, each measurement was performed three times. For each analytical run, final melting temperature of ice ($T_{m,ice}$) and hydrohalite ($T_{m,hh}$), the CO_2 triple point ($T_{t,CO2}$), clathrate dissolution temperature ($T_{m.Clath}$) and the homogenization temperature (T_h) was identified. For interpretation, only results are taken for which the triplet measurements shows a deviation of <0.1 °C for $T_{m,ice}$, $T_{m,hh}$, $T_{t,CO2}$, $T_{m,clath}$ and <1 °C for T_h. As a known feature in unconformity related hydrothermal vein type deposits, a minor amount of fluid inclusions shows metastable behaviour of hydrohalite (complete absence or hydrohalite disappeared above the 0.1 ^{o}C peritectic of NaCl-H_2O). The metastable data and data for which post-entrapment modifications cannot strictly be ruled out are directly excluded from any interpretation and further consideration, and are also not presented in the electronic supplement. Liquid-Vapor fractions are noted for each fluid inclusion. Pressure correction was carried out via the HOKIEFLINCS_H2O-NACL excel based quantification tool of Steele-MacInnis et al. (2012) with estimated 1000 m overburden at the time of fluorite formation (Gotzinger et al., 2005).

To shed light on internal textural variation of host minerals that contain the analyzed fluid inclusion assemblages, cathodoluminescence

imaging was regularly applied for different host phases (fluorite, quartz and calcite). It is important to note, that cathodoluminescence imaging was always done after microthermometry to avoid radiation damage on the fluid inclusion (e.g. Kolchugin et al., 2016, 2020; Kreissl et al., 2018; Epp et al., 2019; Mueller et al., 2020, 2022a, 2022b). A 'hot cathode' CL device (type HC1-LM) at the University of Tübingen was used for imaging. Imaging was done with an acceleration voltage of ~14 kV and a beam current density of ~9 μA mm^{-2} on the sample surface.

3.3. Microraman

The phase composition of individual fluid inclusions was analyzed at Karlsruhe Institute of Technology (KIT), using a Bruker Senterra Raman spectrometer coupled with an Olympus BX51 optical microscope. Prior to each measurement, the Raman spectrometer was calibrated using a neon emission line, and instrument stability was routinely verified through repeated measurements on gem-quality quartz standards to monitor for any signal drift. For fluid inclusions hosted in sphalerite, a 532 nm green laser with a power of 10 mW was employed. The laser spot size was approximately 1 μm, with an accumulation time of 20 s per scan, and the analyses were conducted using a 100× objective, achieving a spatial resolution of ~1 μm on the sample surface. The same laser wavelength (532 nm green laser) was used for analyzing inclusions in fluorite, but with an increased laser power of 20 mW; all other parameters remained consistent with those used for sphalerite.

Raman spectra were collected under ambient conditions, with a spectral resolution of 1.3 cm^{-1} across a wavenumber range of 0–4000 cm^{-1}. Each fluid inclusion was measured as a depth profile, and analytical reliability was ensured through replicate measurements of individual inclusions. Baseline corrections were performed using Fityk software, and the processed spectra were subsequently plotted in Origin.

3.4. Crush-leach analysis

Two fluorite, one baryte and six quartz samples with only one dominant fluid type were selected for bulk crush leach analysis at the LERA facilities of KIT (Ladenburger et al., 2020; Mueller et al., 2020; 2021; Rddad et al., 2025). About 2 g of the roughly crushed sample material with a grain size of >1.0 mm were hand separated under the binocular. Visible impurities are removed from the sample material. Afterwards, the hand separated impurity-free sample material was cleaned for 3 h in ultrapure HNO_3 at 60–70 °C. After temperature treatment in acid, the samples were cleaned for a further week in ultrapure water, exchanging the cleaning liquid at least twice a day. These cleaned samples were dried at 70 °C and crushed to a fine powder in an agate mortar. For each kind of host mineral, separate mortars are used to avoid cross contamination. After crushing, twenty ml of MilliQ water was added to the cleaned sample powder in the agate mortar from which a 10 ml aliquot was used for ion chromatography and for ICP-MS analysis, respectively. To supress doubly-charged cations adsorption on surfaces, the sample aliquot was acidified with 10 μl suprapure HNO_3 (Köhler et al., 2009; Ladenburger et al., 2020). Following the acidification step, the pre-treated and loaded solution was directly injected into a Methrom 930 Compact IC Flex chromatography system equipped with a 858 Professional Sample Processor and a Metrosep A Supp 5 column for quantification of anions (F, Cl, Br, J, NO_3, PO_4 and SO_4). During sample injection of the solutions into the Methrom 858 Professional Sample Processor, disposable syringe filters are used to avoid injection of solid particles in the leachate into the device (CROMAFIL©Xtra RC-20/25 for anions; Ladenburger et al., 2020). On a regular basis, blank runs were performed before and after each individual sample analysis and intercalated defined standard solutions were measured to monitor reproducibility and precision. For the analyses of this contribution, uncertainties are below 10 % and effective detection limits were typically below 10 mg/l.

Trace element analyses of the aliquots were measured with ICP-MS (iCAP RQ, Thermo Fisher Scientific) at the LERA facilities of KIT. The ICP-MS device is equipped with a collision cell to eliminate polyatomic clusters. For calibration, multi-element standard solution (Merck, Certipur) were measured. This procedure is also used for regular quality checks. ^{103}Rh and ^{115}In were used as internal standards for all measurement runs. The certified reference water CRM-TMDW-A (High-Purity standards. Inc.) was chosen to monitor precision and accuracy. Detection limits are provided in the electronic supplement ES2. In the given contribution, accuracy was always between 1 % and 3 %. It is important to note, that no absolute element contents in the ES2 are presented because of the dilution by the crush leach method. For this contribution, no salinity-corrected absolute concentrations in the fluids are determined. It is important to note that due to the likely mixing of multiple fluids, the absolute elemental concentrations derived from the crush-leach method represent averages and do not reflect the composition of a single source or fluid. However, elemental ratios such as Cl/Br and Rb/Cs are considered good tracers of fluid provenance because they are less affected by mixing processes.

4. Results

4.1. Petrography and fluid petrography

All studied samples are fluorite-baryte- (±siderite/calcite)-quartz veins with modal amounts of gangue and ore minerals being strongly variable. For example, samples from the Uburu mine contain up to 90 % baryte, while Enygba samples contain <5 % baryte. Samples from Ikwo are especially rich in galena and sphalerite is very massively developed. At Ameta and Enyigba, Qtz I occur as anhedral fine-grained selvages. Such selvages are absent at the other locations. Only the samples from Otim Land contain an early purple fluorite. All locations contain a massive euhedral fluorite generation which is overgrown by euhedral quartz II and massive or euhedral baryte. At Ameta and Otim Land, late stage euhedral siderite overgrows quartz II. At Enyigba, late-stage calcite is present. All samples contain galena, sphalerite, chalcopyrite and pyrite in fluorite II and quartz II, with tennantite only observed at Ububra. With exception of quartz I, all samples contain primary, pseudosecondary and clusters of fluid inclusion assemblages. Fluids in baryte are not considered further as the fluid inclusions typically decrepitate during microthermometry experiments. For details on the paragenetic sequence see Fig. 4.

4.2. MicroXRF

MicroXRF element mapping was done on all samples to shed light on the interaction between the hydrothermal veins and the country rocks. All MicroXRF element mappings (Fig. 5) show only minor interaction with the country rocks and only mm to cm sized silification on the wallrocks (selvages labelled as quartz I in Fig. 4). Behind the quartz I selvages, feldspars are fresh and unaltered. The so formed selvages are the oldest stage of the hydrothermal veins. On top of the selvages, bands of sulfides (Ccp, Gn, Py) are precipitated and alternate with bands of gangue of Brt, Flr and Qtz. Only in Ameta and Otim Land samples, late stage siderite is recorded. Moreover, the MicroXRF mapping for all locations do not provide evidence for significant element zonation or multiple generations of ore minerals (see represenative mappings in Fig. 5).

4.3. Microthermometry

Fluid inclusions in quartz, sphalerite and siderite have sizes between 5 and 30 μm, whereas fluid inclusions in fluorite can be up to 50 μm large. Liquid-vapor ratios of all studied fluid inclusions are around $L_{95}V_{05}$. Only homogenization to the liquid phase was observed (Fig. 6). Fluid inclusions that show evidence of post-entrapment modifications (e.g., leakage, necking down) and metastable behaviour were excluded

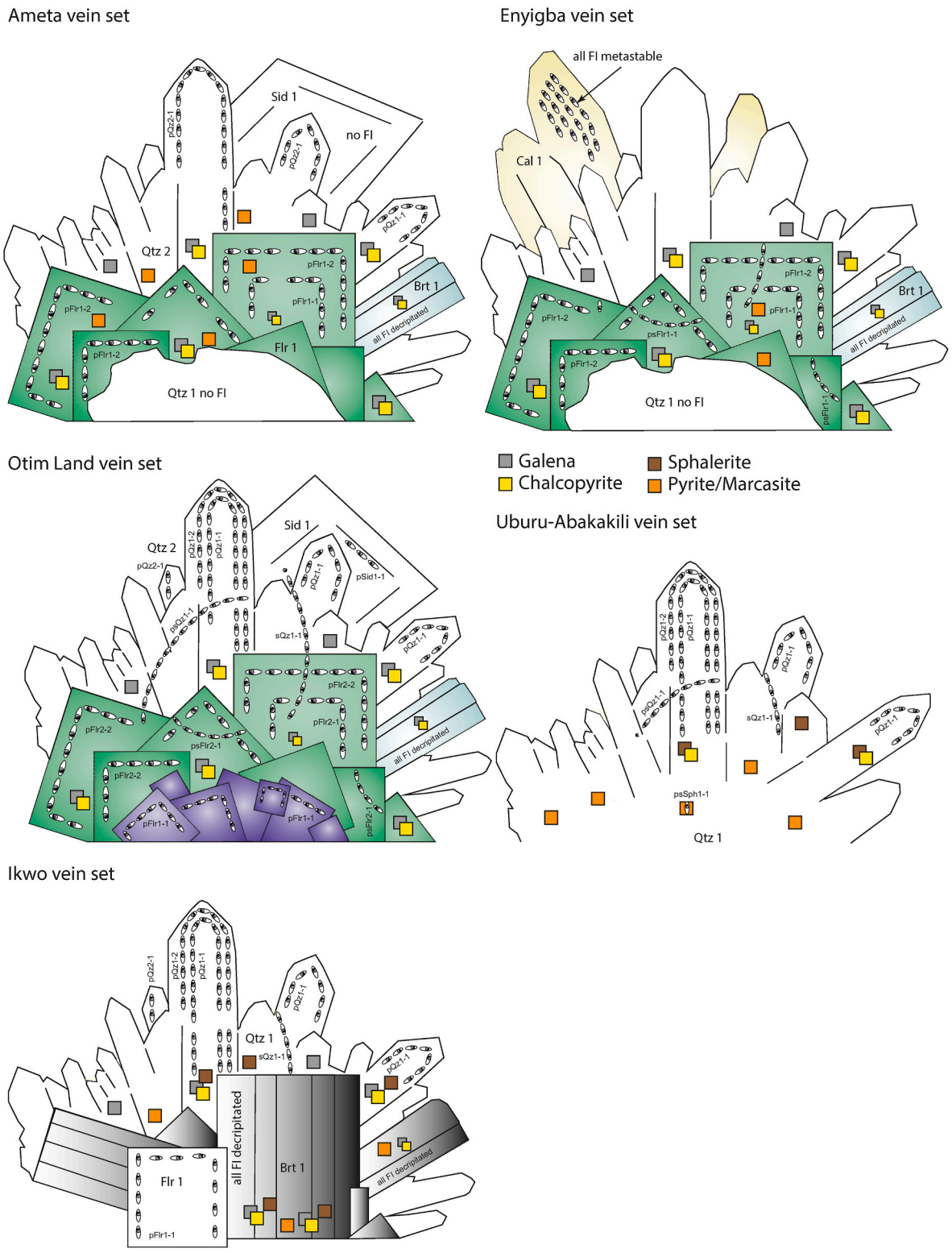

Fig. 4. Schematic sketches of the hydrothermal vein sets studied within this contribution. Note strong similarity between the locations. Only at Uburo no fluorite was recognized.

from analysis and interpretation. The data for each location is very comparable and summarized in Table 1. Only the Enyigba vein system shows elevated temperatures between 196 and 375°C compared to the other studied locations that scatter between 95 and 189 °C. Salinity in primary fluid inclusions is homogeneous between 18.3 and 24 wt% $NaCl + CaCl_2$ (Fig. 7).

Note, the salinity and homogenization temperatures of these inclusions are comparable to those documented in secondary hydrocarbon-bearing inclusions in Arufu calcite and Akwana fluorite, as reported by Akande (1988, 1989).

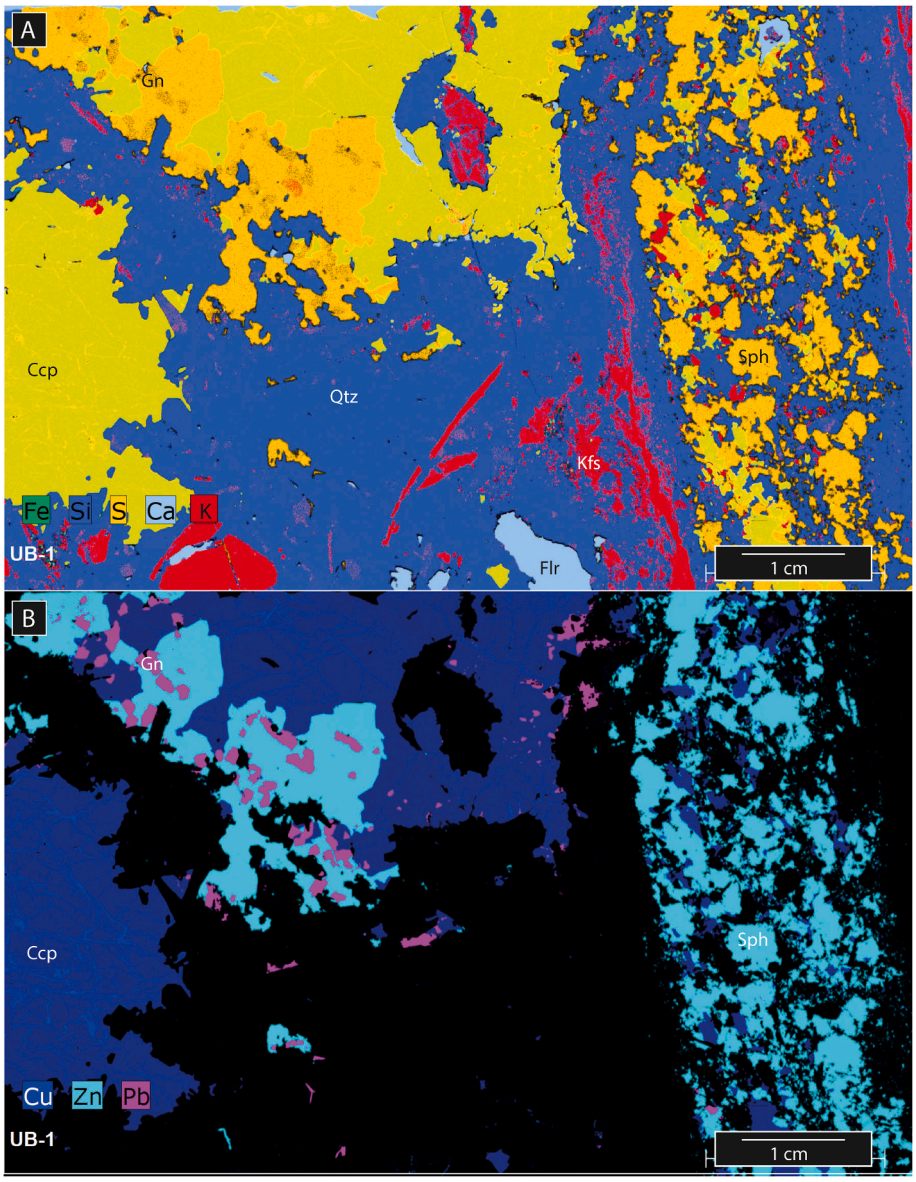

Fig. 5. Exemplary MicroXRF map of the hydrothermal veins at Ububra district. Base metal mineralization is widespread and strongly intergrown with quartz and fluorite. The domain does not show strong evidence of a hydrothermal overprint on the country rock granite (host of the feldspars).

4.4. Crush leach analyses

The bulk crush leach analyses show for the Enyigba fluorite samples Cl/Br ratios of 195 and 208 (below the seawater ratio of 288), and Rb/Cs ratios of 9.9, respectively (Fig. 7). The samples from the Uburu district, however, contain Cl/Br ratios always above the sea water ratio with a scatter between 446 and 3790. The Rb/Cs ratios are higher compared to Enyigba samples and scatter between 12 and 21.6. The sample studied from Ameta (AM samples) shows a Cl/Br ratio of 482 and a Rb/Cs of 14.4. At Ikwo, Cl/Br scatter between 317 and 1740 with Rb/Cs values between 0.3 and 7.5. The samples from Otim Land (OT) have Cl/Br between 770 and 2720 with a Rb/Cs ratio of 3.6–17.9. The complete data set is presented in the electronic supplement (ES2). Other element ratios were considered (see electronic supplement), but do not show any systematics.

4.5. Microraman

Raman spectroscopic analysis was conducted on forty fluid inclusions hosted within sphalerite and fluorite. Only the data of the representative fluid inclusions is presented in Fig. 8A and B. Bands observed at 1072 and 1152 cm^{-1} indicate the presence of sulfur dioxide (SO_2) and C–H stretching vibrations, respectively, suggesting an organic or hydrocarbon component within the inclusions. Additional bands at 1792 and 2355 cm^{-1} are attributed to carbon dioxide (CO_2), while a broad band at 3392 cm^{-1} corresponds to H_2O, likely due to O–H stretching. Notably, no H_2S-related peaks were detected, which may imply that all available sulfide (S^{2-}) produced via sulfate reduction was either consumed in sulfide mineral precipitation or converted into gaseous SO_2.

Secondary fluid inclusions in fluorite were also analyzed. Peaks at 272, 311 and 322 cm^{-1} are typical of fluorite. Bands at 1072, 1823 and 1852 cm^{-1} further support the presence of hydrocarbon species within the fluid phase. These secondary inclusions in fluorite appear to be genetically related to those in sphalerite, based on similarities in both homogenization temperature and fluid composition.

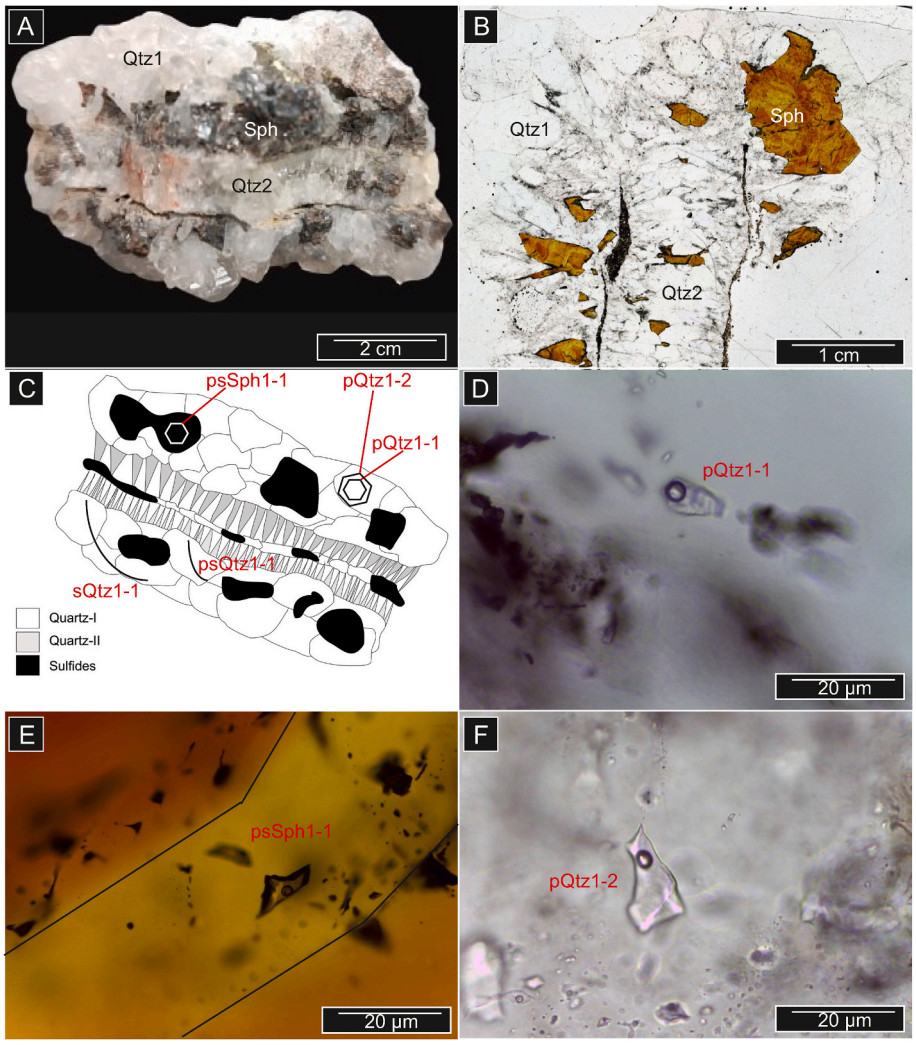

Fig. 6. (A) Hand specimen of UB sample, (B) thin section scan of the same sample, (C) sketch of (A) showing the various quartz generations and fluid assemblages, (D) primary fluid inclusions in quartz 1, (E) sphalerite from the same sample UB, the light colour sphalerite allowed for the identification of fluid inclusions without any IR spectroscopy, and (F) primary fluid inclusions in quartz. (For interpretation of the references to colour in this figure legend, the reader is referred to the Web version of this article.)

5. Discussion

5.1. Fluid provenance and precipitation process

The fluid composition from the different vein sets (with exception of Enyigba) show a mixing line between a hot (>190 °C) NaCl-dominated fluid (endmember 1) with a salinity of ~22 wt% NaCl + $CaCl_2$ and a low temperature (<90 °C), Na-Ca fluid (up to 50 % Ca; endmember 2), with a slightly lower, but clearly distinguishable salinity of ~18.3 wt% NaCl + $CaCl_2$. The trends appear much clearer in the Na/(Ca + Na) versus salinity and Th plots as well as in the Na_{excess}-$Ca_{deficite}$ plots (Fig. 7C). Since the samples of Enyigba are always in the extrapolation of the alignment of the fluid datapoints from all other locations, the high temperatures are most likely reflecting a strong shift in the mixing ratio towards the deep-seated endmember. As shown for other places in the world via S-isotope systematics, temperatures of ~350 °C are likely the reservoir temperatures of the deep-seated basement brines above the brittle-ductile transition zone (e. g., Schwinn et al., 2006). Since the Benue Trough as an aulacogen still has an increased heatflow, the observed high temperatures can be explained by the geological setting.

The observed fluids are very similar to those from Mesozoic fluorite veins of central Europe and northern and southern Africa (e.g. Boiron et al., 2010; Burisch et al., 2016a; 2017a, b; Keim et al., 2019; Haschke et al., 2021; Burisch et al., 2022; Rddad et al., 2024a,b; Walter et al., 2024), for which mixing between a deep-seated NaCl-brine (20–25 wt% salinity) and a high salinity limestone-derived, Ca-enriched fluid (almost equal salinity) is assumed to have caused fluorite (and baryte) deposition (including some veins with base metal mineralization, Burisch et al., 2022 and references therein). As evidence of fluid boiling is lacking and fluid cooling is an insignificant process for fluorite and baryte precipitation (Walter et al., 2019), fluid mixing best explains the observed data. Moreover, as the solubility products of fluorite and baryte are very low (pK_{sp} ~ 10.60 and pK_{sp} ~ 9.97, respectively; Ball and Nordstrom, 1991), a common transport of Ca-Cl-complexes and F^- as well as Ba-Cl-complexes and SO_4^{2-} in a single fluid is essentially impossible. Burisch et al. (2016a,b) provided strong experimental evidence, that Ba and F are leached from crystalline basement via desiccation reactions under greenschist facies conditions (Brockamp and Clauer, 2005; Walter et al., 2019; Jungmann et al., 2025), in contrast to formation waters, which are limestone-derived and which can provide Ca and SO_4 (Bons et al., 2014; Walter et al., 2016, 2017a, 2019; Jungmann et al., 2025 and references therein). Although the mixing of Ca-SO_4 and Ba-F-rich brines adequately explains the precipitation of fluorite and baryte, the presence of sulfide mineralization requires an additional mechanism to create reducing conditions.

To explain the nests and layers of sulfides, episodic influx of reduced

Table 1
Summary of the fluid inclusion analyses.

Locality	samples	FI Assemblage	Tm,ice °(C)	Tm,hh (.)	Th (.)	Salinity (wt.% NaCl + $CaCl_2$)
Enyigba	EN	pFl1-1, pFl1-2	−18 to −23	−22 to −23.5	375 to 355	20.6 to 24.1
		sFl1-1	−9 to −13	−25 to-27.5	217 to 196	13.0 to 16.6
Ameta	AM	pFl1-1, pFl1-2	−15.4 to −19.1	−26.9 to −28.1	123 to 128	18.3 to 20.7
		pQtz2-1	18.8 to −21.1	−26.3 to −28	99 to 108	21.4 to 22.0
Uburu	UB	pQtz1-1, pQtz1-2	−16 to −20	−23 to −26.5	163–189	18.9 to 22
		psQtz1-1	−17 to −20	−22 to −24	172 to 187	19.8 to 22
		sQtz1-1	−6 to −20	−22 to −28.5	135 to 189	3.6 to 22
		psSph1-1	−16 to −22	−22 to −25	162 to 177	19.1 to 21.8
		sSph1-1	−9 to −20	−22 to −29	131–177	13 to 21.8
Otim Land	OT	pQtz1-1	−18 to −20.8	−25.3 to −28.6	119 to 143	20.1 to 21.9
		pQtz2-1	−16.9 to −20	−25.6 to −28.6	119 to 134	19.3 to 21.4
		pFl1-1 to pFl1-2	−15.3 to −19	24.9 to −29.2	131 to 149	18.2 to 20.6
		pSid1-1	−10 to −14.5	−28.9 to −30.5	95 to 105	14.0 to17.7
Ikwo		(pQtz1-1)	18.4 to −21	−24.9 to −28.6	110 to 121	20.4 to 22
		pQtz2-1	−19.3 to −21.3	−24.5 to −28.4	100 to 116	21 to 22.2
		pQtz2-2	−8.7 to −11	−26.5 to −28.4	92 to 100	12.8 to 14.9

fluids is required, as this can lead to sulfide precipitation instead of baryte. Indeed, the presence of hydrocarbons in the fluids is shown by MicroRaman results (see result chapter). A very rough mass balance estimation provided by Walter et al. (2019) on the hydrothermal system in the Schwarzwald (Germany) implies that only a very minor influx of CH_4 is required during fluid mixing to precipitate galena (~0.01 mmol) or sphalerite (~0.03 mmol) from 1 L of the mixed fluid (containing 2 ppm Pb or Zn). Since reducing agents are available by the oilfield fluids in the southern and northern Benue Trough, the tiny amount of the reducing agent is easily available in the area to shift the physicochemical parameters from the sulfate into the sulfide stability field. As the availability of the reducing agent is most likely the limitation of quantitative sulfate reduction, the mixed fluid parameters shift back after sulfide precipitation (producing sulfide zones or nests in the baryte veins).

The Benue Trough and the Niger Delta hosts significant hydrocarbon resources (and related oilfield brines) that have been intensely explored and which have been under long term exploitation (e.g. Abubakar, 2014). Such hydrocarbons are rich in organic material, CH_4 and H_2S and therefore have a great potential to act as reducing agent which is required for hydrothermal sulfide mineralization in the veins of Nigeria (e.g. Kolchugin et al., 2016, 2020). Since veins hosted in the Middle Benue Trough are sulfide-barren, and only veins hosted in the vicinity of the Northern and Southern Benue Trough contain sulfides at all, there seems to be a clear link to the oil fields which are also discovered only in Southern Benue Trough/Niger Delta and in the Northern Benue Trough. This is also reflected by the presence of a redox agent in the Raman analyses of this contribution. Therefore, unconformity-related hydrothermal veins in the northern and southern Benue Trough have a high potential for base metal mineralization, whereas high grade fluorite and baryte can be expected in the veins of the Middle Benue Trough.

5.2. Deposit model

To understand hydrothermal processes in the basement, Ca_{excess}-$Na_{deficite}$ plots (Fig. 7C) have been shown to be a powerful tool (e.g. Mueller et al., 2024; Kreissl et al., 2018). The Ca_{excess}-$Na_{deficite}$ discrimination diagram provide strong evidence against a single bittern brine origin for all samples (including Enyigba location) and rather direct towards an original seawater source. Gravity-driven downwards-migrating seawater can dissolve pre-existing halite deposits from sedimentary sequences. For European and African fluorite deposits, the development of a basement brine is brought into context to the first surficial deposition of evaporates (e.g. Walter et al., 2016, 2017, 2019, 2024, Burisch et al., 2022; Rddad et al., 2022, 2024, 2025 and references therein). For the Benue Trough in Nigeria, evaporite formation during Albian time (113–100.5 Ma; Tijani, 2004) represents the lower age limit of halite dissolution brine formation.

The Cl/Br ratio in fluids is also a powerful tool to decipher their source of salinity (Cl/Br = 288: seawater; Cl/Br > 288: halite dissolution; Cl/Br < 288: halite precipitation during seawater evaporation → bittern brine formation; Böhlke and Irwin, 1992; Stober and Bucher, 2004; Seo et al., 2011; Fusswinkel et al., 2013; 2014; Scharrer et al., 2023; Walter et al., 2016, 2017 and references therein). In principle, high salinities can be reached by clay mineral formation in the basement rocks underlying the Benue Trough (desiccation). However, this process alone cannot explain the variable and high Cl/Br ratios in the fluid which clearly show the influence of halite dissolution (Fig. 8; Burisch et al., 2016a). Nevertheless, for Enyigba samples desiccation processes could lead to the Cl/Br ratio below the seawater value (Fig. 7, Cl/Br 195 and 208) and to the observed high salinities (Tijani, 2004). A different process to develop the observed deep-seated, highly saline brines could be the infiltration of surficial shallow fluids (e.g., marine or meteoric waters) to deep domains of the basement. At depth, they may also acquire an elevated salinity due to potential fluid-rock interaction and desiccation processes. Experimental data of Burisch et al. (2016a), however, indicate that very high salinities cannot simply be developed by progressing desiccation processes in the crystalline basement (for the experiments crushed material was used with a high reaction surface comparable to those of a cataclastic shear zone which therefore overestimates the role of desiccation in the upper crust). Hence, common superficial fluids (e.g. meteoric water that has descended into the basement/unconformity) can be widely excluded as potential source for fluid endmembers 1 and/or 2 (even for secondary fluid inclusions, which indicate a dilute fluid), as the salinity of such superficial fluids is significantly too diluted. This bittern brine is in strong chemical disequilibrium and starts to react with the basement rocks (alteration of mica and feldspar of the crystalline basement). Since microXRF mapping shows fresh feldspars and micas at the precipitation level, basement leaching must happened at deeper crustal levels as already indicated by e.g. Burisch et al. (2016a,b) or Jungmann et al. (2025). Clay minerals and secondary albite are formed as a consequence of alteration under greenshist facies conditions. This brine-basement interaction is reflected by the data trend of 1 Ca for 1 Na exchange in Fig. 7C. Moreover, this trend indicates albitization to be the major process of basement alteration (Kreissl et al., 2018 and references therein). Burisch et al. (2016b), Walter et al. (2019), Kluge et al. (2024) and Jungmann et al. (2025) have provided strong evidence that basement alteration leads to a significant release of trace elements like Ba, F and metals like Cu, Pb, Zn into the hydrothermal fluid as the secondary minerals usually do not have the crystallographic capacity to incorporate those trace elements in equally high amounts (Walter et al., 2019).

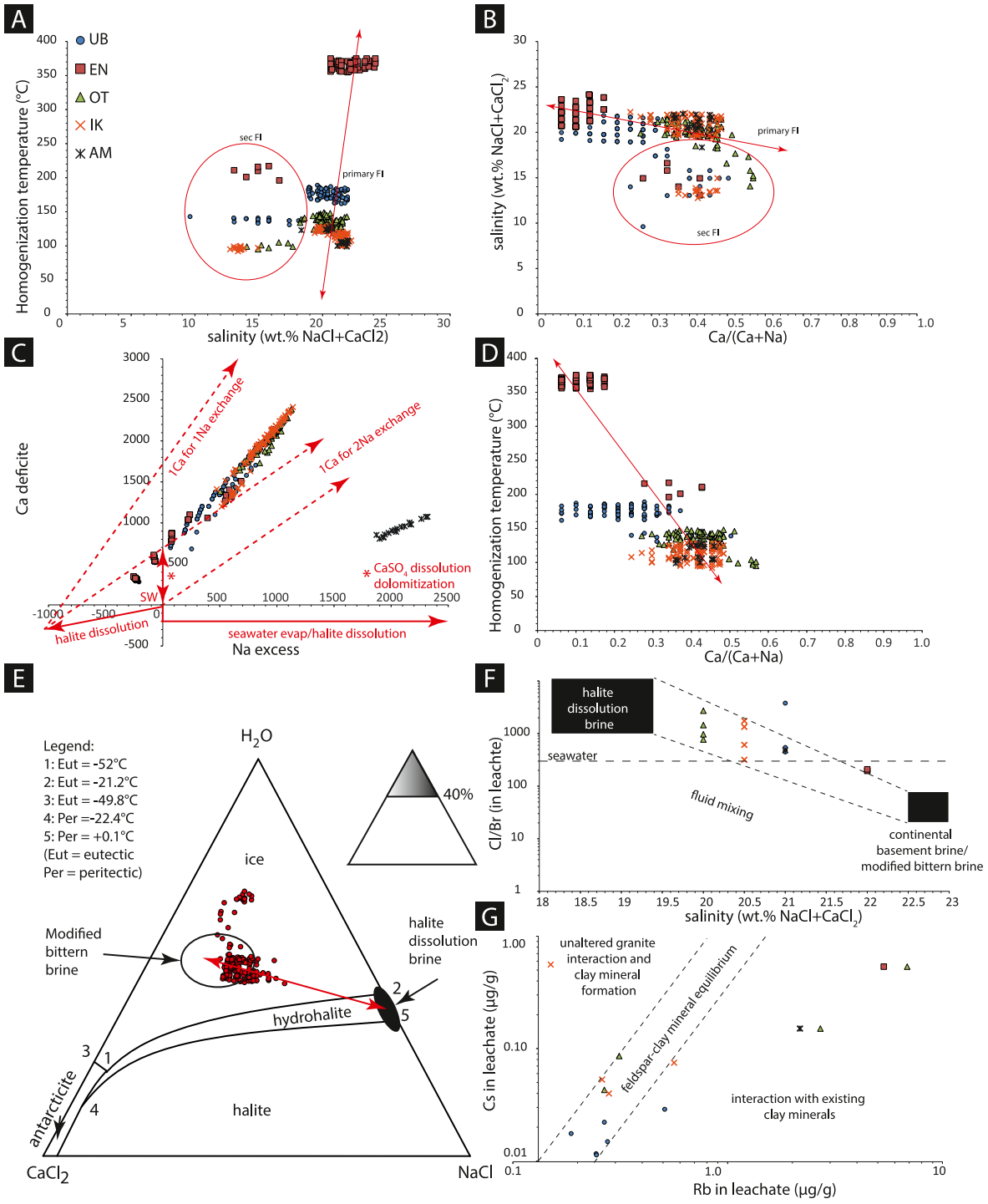

Fig. 7. A) Homogenization temperatures versus salinity. Note the systematic higher temperatures of the EN samples. B) Salinity versus molar Ca/(Ca + Na) ratio. Note primary fluid inclusions follow a trend line. Only secondary and pseudosecondary deviate from the primary trend line. C) Ca deficite, Na excess plot illustrates that the FI data follow a basement interaction trend after halite dissolution. D) Homogenization temperatures versus molar Ca/(Ca + Na) ratio. E) Ternary system NaCl-$CaCl_2$-H_2O indicating a mixing line for primary FI of a halite dissolution brine and a modified bittern brine with a strong modified bittern brine component. F) Cl/Br mass ratios versus salinity. Note: all data plot on a mixing line between a halite dissolution brine and a modified bittern brine. Rb versus Cs plot shows that that most bulk fluid compositions plot in the fields of feldspar-clay mineral equilibrium and interaction with existing clay minerals.

Endmember fluid 1 likely leached the crystalline basement rocks of Nigeria for tens of million years. The bittern brine underwent desiccation processes and caused the alteration and albitization of the primary minerals of the basement rocks, which again lead to chemical modification of the brine and the release of trace elements (in particular base metals) into the fluid, which than would reflect a modified bittern brine (Bons et al., 2014). After the first infiltration of the basement with bittern brines, Ca- and SO_4-enriched connate fluids formed in the limestone formations of the Asu and Nkalagu Groups (endmember 2). The now subsurficial halite deposits/sequences are dissolved by influx of marine/meteoric fluids and form dense halite dissolution brines (elevated in Cl/Br above seawater, see Fig. 7F) and also start to migrate downwards (most likely desiccation driven; Bons et al., 2014). Until opening of the South Atlantic Ocean (Pangaean rifting; ~134-80 Ma,

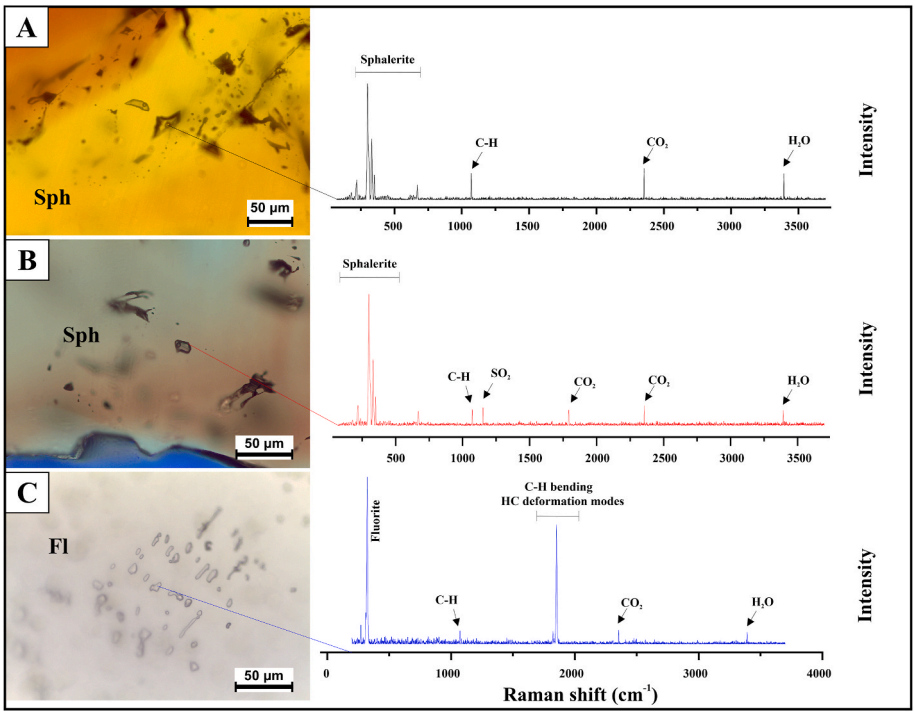

Fig. 8. A) Exemplary Raman spectra of sphalerite hosted fluid inclusions (sample UB-2). Note detection of SO_2 in sphalerite hosted fluid inclusions as well. B) Exemplary Raman spectra of fluorite hosted fluid inclusions. Note the appearance of C-H bands as an indicator for the presence of hydrocarbons (sampleEN-2).

Channell et al., 1995; Malinverno, 2012; Ogg, 2012) in Jurassic-Cretaceous times, both fluids (endmember 1 and 2) stay in the upper crust as a fluid stratified section (see Stober and Bucher, 2012; Walter et al., 2016 and references therein). Since Cretaceous times, the pathways established in the context of Pangaea rifting enable endmember fluid 1 and 2 to become mobilized and mix occasionally together with fluid 3 which transports the redox agent from hydrocarbon reservoirs of the Benue Trough (probably hydrocarbons). This superregional, rift related fluid mixing event lead to the formation of the hydrothermal fluorite-baryte-quartz veins with and without base metal

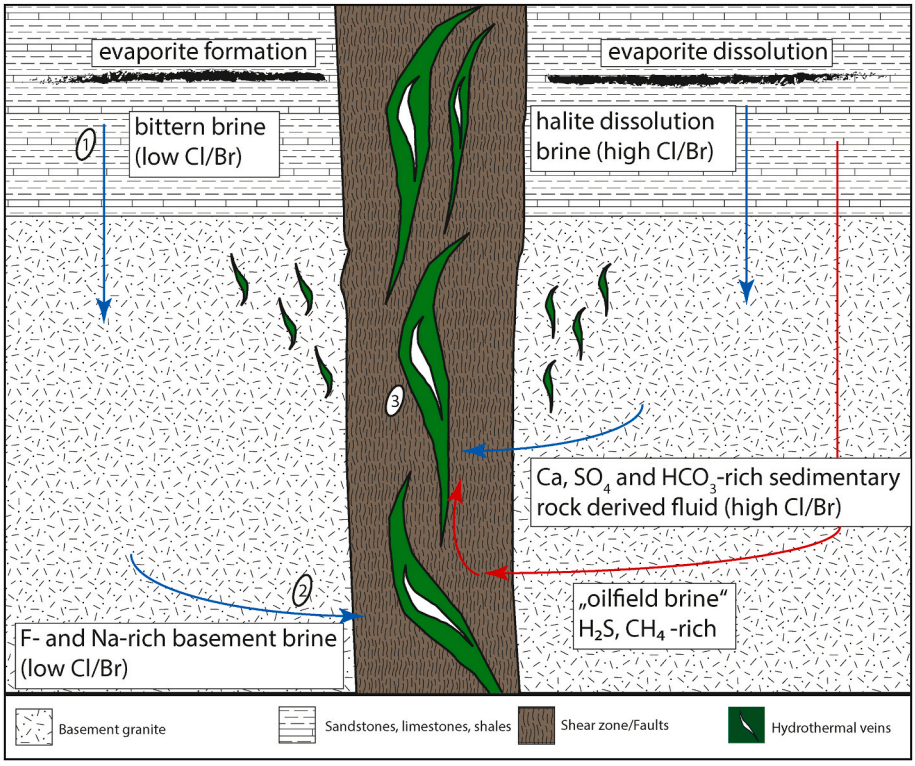

Fig. 9. Schematic model of unconformity-related hydrothermal vein type formation in the Benue Trough. 1) Formation and downward migration of bittern brine. 2) The opening of fractures causes the formation of a hydraulic head that sucks fluids into the structure. 3) Fluid mixing and precipitation.

ores along the Benue Trough (Fig. 9).

If this model is correct, reduced brines including mobilized hydrocarbons were transported from bituminous formations associated with the oil reservoirs in Nigeria (e.g. Abubakar, 2014). Such "oilfield brines" (fluid 3) migrate downwards, driven by a desiccation-induced hydraulic head (following the "mixing from below model" of Bons et al., 2014) into the crystalline basement of the Benue Trough. A potential contrasting process could be triggered by rift tectonics and the related establishments of pathways in the context of hydrocarbon pressure subtracting the reservoir hydrostatic pressure, pressure attenuation, and displacement pressure (see Lao et al., 2019 for details). Once the major fracture network has been established as a far field consequence of Pangaea rifting, all three fluids (endmember 1, endmember 2 and the redox agent carrying fluid 3) can be sucked into the newly opened fractures that formed the Benue Trough hosted vein-type deposit (above the unconformity separating the crystalline basement from the sedimentary overburden as it is common at numerous other places in Europe and Africa). In the last-named scenario, endmember fluid 1 and 2 ascend together with the redox agent carrier fluid (fluid 3) and mix at the deposit level.

Rubidium/Cs ratios are a powerfull tool to decipher water rock interaction processes, desiccation and clay mineral formation in basement rocks and interaction with shales (Burisch et al., 2016a,b). The Rb/Cs ratio serves as an effective tracer in this context, as both rubidium (Rb) and cesium (Cs) typically substitute for potassium (K) in primary rock-forming minerals, but fractionate during the formation of clay minerals. Rb is incorporated into the crystalline structure of clay minerals, whereas Cs tends to be adsorbed on the surfaces of clays (Göb et al., 2013 and references therein). This distinction leads to fractionation within the fluid phase. As a result, the Rb/Cs ratio of a fluid can be modified by the alteration of feldspars and biotite into clay minerals (Aquilina et al., 1997; Göb et al., 2013, and references therein). Consequently, fluid Rb/Cs ratios of less than 2 are indicative of fluids that have interacted with unaltered crystalline rocks, while ratios near 2 correspond to equilibrium conditions during the alteration of primary minerals to clay minerals. Ratios greater than 5 suggest water-rock interactions involving pre-existing clay minerals, without alteration of primary phases (Göb et al., 2013). The high Rb/Cs ratios recovered by bulk crush leach analyses indicating that fluids of all host minerals interact with existing clay minerals (Fig. 8B and C) and therefore a fluid component at the crustal level of deposit formation is likely since numerous of the veins are hosted by shales (Fig. 9).

This multicomponent fluid mixing process can lead to excessive and immediate precipitation of fluorite, baryte and locally sulfides where the redox agent (fluid 3) is present. As long as the fluid mixing process continues, the main ore stage is deposited. After the short-living fluid batch has been homogenised, the remaining fluid still resided in the open cavity of the vein (open appearance evidenced by the presence of euhedral quartz and siderite). During cooling of the fluid batch accompanied by dilution (reflected in the salinity versus T_h diagram, Fig. 7A), quartz and occasionally siderite (only at parts of Otim Land) were precipitated. Since the samples do not provide any evidence for multiple reactivations of pathways (e.g. brecciation, etc …), like it is known from Central Europe (e.g. Dill et al., 2011; Keim et al., 2019; Walter et al., 2019), there seems to have been only one single period in time during which the Nigerian vein-type deposits formed.

Combining the geochemical arguments of this study with field observation show that mineralization in the study area does not exhibit a clear local distribution trend, but follows a regional NE-SW orientation, aligning with the basin's main axis. The host rocks include Albian Shales (Asu-River Group), Turonian sandstones and shales (Eze-Aku Group), and Post-Turonian to Coniacian intrusive bodies (e.g., at Enyigba) whereas mineralization shows no strong lithologic preference. Despite the proximity of the basement-sedimentary cover unconformity, field observations clearly show that mineralization is structurally controlled and related to sedimentary basin dynamics (subsidence and depo center formation) and rift related structures, primarily confined to parallel or sub-parallel en-echelon NW-SE fractures, which appear younger than the dominant NE-SW trend formed during the onset of the rifting (Oha et al., 2017) and likely during an intensive compressional stress event during Santonian times (Yenne et al., 2025). Veins vary in size from a few centimeters to over 2 km in length, with mineral compositions differing by location whereas base metal mineralization is more prominent in areas where hydrocarbon systems are known. Therefore, the southern deposits are polymetallic (dominated by galena, sphalerite, and chalcopyrite), while the northern deposits show high purity baryte and fluorite (Oha et al., 2017). From an exploration point of view, most fertile areas for base metal mineralization are those where the basement-sedimentary cover unconformity is shallow and NW-SE and N-S structures dominate, and hydrocarbon systems overlap with the last-named structure framework.

6. Conclusions

The unconformity-related hydrothermal vein type deposits in Nigeria developed in the context of Pangaea break up and opening of the southern Atlantic Ocean. After surficial halite precipitation, a bittern brine formed that descended and reacted with the crystalline basement rocks, leaching Ba, F, and base metals. Subsequently, meteoric or marine fluids percolated through the area and partly dissolved the existing evaporite sequences forming a halite dissolution brine rich in SO_4 and Ca. Both high salinity brines were stored in the crystalline basement until pathways opened as a result of Pangaea rifting and mixing between them caused massive formation of fluorite-baryte-quartz veins with base metals presence as a consequence of episodic influx of reduced oilfield brines. This model not only elucidates the genesis of Nigerian deposits but also establishes a robust exploration criterion: association with known hydrocarbon systems serves as a key indicator of base-metal enrichment in comparable unconformity-related settings. Future studies that employ direct geochronological analyses of vein minerals are required to constrain the timing of the Nigerian vein formation event (s) relative to the stages of Atlantic rifting.

CRediT authorship contribution statement

Benjamin F. Walter: Writing – review & editing, Writing – original draft, Visualization, Validation, Supervision, Resources, Project administration, Methodology, Investigation, Data curation, Conceptualization. **Ndukauba Egesi:** Writing – review & editing, Writing – original draft, Methodology, Funding acquisition, Conceptualization. **Mohsin Raza:** Writing – review & editing, Writing – original draft, Visualization, Validation, Methodology, Investigation, Funding acquisition, Data curation, Conceptualization. **Micheal Agbebia:** Writing – review & editing, Investigation, Data curation. **Fadila Adamu:** Writing – original draft, Visualization, Investigation, Conceptualization. **R. Johannes Giebel:** Writing – review & editing, Writing – original draft, Visualization, Validation, Project administration, Investigation, Funding acquisition, Data curation, Conceptualization. **Michael A.W. Marks:** Writing – review & editing, Writing – original draft, Validation, Supervision, Conceptualization. **Emmanuel Chidi Ugbaja:** Writing – review & editing, Investigation, Data curation. **Gregor Markl:** Writing – review & editing, Writing – original draft, Supervision, Resources, Project administration, Funding acquisition, Conceptualization.

Declaration of competing interest

The authors declare the following financial interests/personal relationships which may be considered as potential competing interests: Mohsin Raza reports financial support was provided by Higher Education Commission of Pakistan (HEC Pakistan). Mohsin Raza reports financial support was provided by German Academic Exchange Service. Mohsin Raza reports financial support was provided by Graduate School

for Climate and Environment (GRACE). Mohsin Raza reports financial support was provided by Karlsruhe House of Young Scientists (KHYS). If there are other authors, they declare that they have no known competing financial interests or personal relationships that could have appeared to influence the work reported in this paper.

Acknowledgments

We thank t the Higher Education Commission of Pakistan (HEC Pakistan) and the German Academic Exchange Service (DAAD), Graduate School for Climate and Environment (GRACE) and Karlsruhe House of Young Scientists (KHYS) for financial support of Mohsin Raza. The authors thank Elisabeth Eiche, Claudia Mössner, Maya Denker, and Kristian Nikoloski from the LERA facilities at KIT for their valuable assistance in the analysis and material preparation. Field expeditions logistics to collect samples and export to Germany was provided by Chidi Ugbaja an MSc Student at the University of Port Harcourt. We would like to express our sincere gratitude to two anonymous reviewers and the associate Editor, Dr. Harald Dill, for their insightful comments and suggestions that improved the quality of this manuscript. We also thank the Editor-in-Chief, Dr. Read Brown Mthanganyika Mapeo, for handling of this manuscript.

Appendix A. Supplementary data

Supplementary data to this article can be found online at https://doi.org/10.1016/j.jafrearsci.2025.105964.

Data availability

All data is provided as electronic supplement.

References

Akande, S.O., Abimbola, A.F., 1987. Aspects of the genesis of the lead-zinc-fluorite-baryte mineralization in the Nigerian Benue Trough. Colloquium on African geology 14, 365–369.
Akande, S.O., Mucke, A., 1989. Mineralogical, textural and paragenetic studies of the lead zinc copper mineralization in the lower Benue Trough (Nigeria) and their genetic implications. J. Afr. Earth Sci. 9 (1), 23–29.
Akande, S.O., Mücke, A., 1993. Coexisting copper sulphides and sulphosalts in the Abakaliki Pb-Zn deposit, lower Benue Trough (Nigeria) and their genetic significance. Mineralogy and PetrologyY-Leoben- 47, 183-183.
Andrew-Oha, I., Mosto-Onuoha, K., Sunday-Dada, S., 2017. Contrasting styles of lead-zinc-barium mineralization in the Lower Benue Trough, Southeastern Nigeria. Earth Sci. Res. J. 21 (1), 7–16.
Aquilina, L., Pauwels, H., Genter, A., Fouillac, C., 1997. Water-rock interaction processes in the Triassic sandstone and the granitic basement of the Rhine Graben: geochemical investigation of a geothermal reservoir. Geochem. Cosmochim. Acta 61 (20), 4281–4295.
Arinze, I.J., Emedo, C.O., 2021. Integrated geophysical investigation for shallow-scale massive (Pb-Zn) sulphide and baryte exploration in the Abakaliki and Obubra Mining Districts (AOMD), Southeastern Nigeria. Mining, Metallurgy & Exploration 38 (1), 381–395.
Banks, D.A., Boyce, A.J., Samson, I.M., 2002. Constraints on the origins of fluids forming Irish zn-pb-ba deposits: evidence from the composition of fluid inclusions. Econ. Geol. 97 (3), 471–480.
Benkhelil, J., 1989. The origin and evolution of the Cretaceous Benue Trough (Nigeria). J. Afr. Earth Sci. 8 (2–4), 251–282.
Böhlke, J.K., Irwin, J.J., 1992. Laser microprobe analyses of Cl, Br, I, and K in fluid inclusions: implications for sources of salinity in some ancient hydrothermal fluids. Geochem. Cosmochim. Acta 56 (1), 203–225.
Boiron, M.C., Cathelineau, M., Richard, A., 2010. Fluid flows and metal deposition near basement/cover unconformity: lessons and analogies from pb–zn–f–ba systems for the understanding of Proterozoic U deposits. Geofluids 10 (1-2), 270–292.
Bons, P.D., Fusswinkel, T., Gomez-Rivas, E., Markl, G., Wagner, T., Walter, B., 2014. Fluid mixing from below in unconformity-related hydrothermal ore deposits. Geology 42 (12), 1035–1038.
Brockamp, O., Clauer, N., 2005. A km-scale illite alteration zone in sedimentary wall rocks adjacent to a hydrothermal fluorite vein deposit. Clay Miner. 40 (2), 245–260.
Burisch, M., Gerdes, A., Walter, B.F., Neumann, U., Fettel, M., Markl, G., 2017a. Methane and the origin of five-element veins: Mineralogy, age, fluid inclusion chemistry and ore forming processes in the Odenwald, SW Germany. Ore Geol. Rev. 81, 42–61.
Burisch, M., Markl, G., Gutzmer, J., 2022. Breakup with benefits-hydrothermal mineral systems related to the disintegration of a supercontinent. Earth Planet Sci. Lett. 580, 117373.
Burisch, M., Marks, M.A., Nowak, M., Markl, G., 2016a. The effect of temperature and cataclastic deformation on the composition of upper crustal fluids—an experimental approach. Chem. Geol. 433, 24–35.
Burisch, M., Walter, B.F., Markl, G., 2017b. Silicification of hydrothermal gangue minerals in pb-zn-cu-fluorite-quartz-baryte veins. Can. Mineral. 55 (3), 501–514.
Burisch, M., Walter, B.F., Wälle, M., Markl, G., 2016b. Tracing fluid migration pathways in the root zone below unconformity-related hydrothermal veins: insights from trace element systematics of individual fluid inclusions. Chem. Geol. 429, 44–50.
Carignan, J., Gariépy, C., Hillaire-Marcel, C., 1997. Hydrothermal fluids during Mesozoic reactivation of the st. Lawrence rift system, Canada: c, O, Sr and Pb isotopic characterization. Chem. Geol. 137 (1–2), 1–21.
Channell, J.E., Erba, E., Nakanishi, M., Tamaki, K., 1995. Late Jurassic-Early Cretaceous Time Scales and Oceanic Magnetic Anomaly Block Models.
Cherai, M., Rddad, L., Talbi, F., Walter, B.F., 2023. Trace-element geochemistry and S–O isotopes in the fluorite-baryte mineralization of Merguechoum, Moroccan eastern Meseta: insights into ore genesis to the pangea rifting. Acta Geochimica 42 (3), 435–452.
Crognier, N., Hoareau, G., Aubourg, C., Dubois, M., Lacroix, B., Branellec, M., et al., 2018. Syn-orogenic fluid flow in the Jaca basin (south pyrenean fold and thrust belt) from fracture and vein analyses. Basin Res. 30 (2), 187–216.
Dill, H., Dulski, P., Möller, P., 1986. Fluorite mineralization and REE patterns in vein-type deposits from the N Bavarian Basement. Neues Jahrb Min Abh 154, 141–151.
Deane, J., 1995. The structural evolution of the Kombat deposits, Otavi Mountainland, Namibia. Communications of the Geological Survey of Namibia 10, 99–107.
Dill, H., 1988. Geologic setting and age relationship of fluorite-barite mineralization in southern Germany with special reference to the Late Paleozoic unconformity. Miner. Deposita 23 (1), 16–23.
Dill, H.G., Weber, B., 2010. Accessory minerals of fluorite and their implication regarding the environment of formation (Nabburg–Wölsendorf fluorite district, SE Germany), with special reference to fetid fluorite ("Stinkspat"). Ore Geol. Rev. 37 (2), 65–86.
Dill, H.G., Hansen, B.T., Weber, B., 2011. REE contents, REE minerals and Sm/Nd isotopes of granite-and unconformity-related fluorite mineralization at the western edge of the Bohemian Massif: with special reference to the Nabburg-Wölsendorf District, SE Germany. Ore Geol. Rev. 40 (1), 132–148.
Dill, H.G., Weber, B., Eigler, G., Kaufhold, S., 2012. The fluorite deposits NE of Regensburg, SE Germany—A mineralogical and chemical comparison of unconformity-related fluorite vein-type deposits. Geochemistry 72 (3), 261–278.
EC 2020a–European Commission, 2020. Critical Materials for Strategic Technologies and Sectors in the EU–a Foresight Study, 2020.
El-Nafaty, J.M., 2015. Rare earth element and stable sulphur (δ 34S) isotope study of baryte–copper mineralization in Gulani area, Upper Benue Trough, NE Nigeria. J. Afr. Earth Sci. 106, 147–157.
Epp, T., Walter, B.F., Scharrer, M., Lehmann, G., Henze, K., Heimgärtner, C., Bach, W., Markl, G., 2019. Quartz veins with associated sb-pb-ag±au mineralization in the Schwarzwald, SW Germany: a record of metamorphic cooling, tectonic rifting, and element remobilization processes in the Variscan belt. Miner. Deposita 54, 281–306.
Ezepue, M.C., 1984. The geologic setting of lead-zinc deposits at Ishiagu, Southeastern Nigeria. J. Afr. Earth Sci. 2 (2), 97–101, 1983.
Farrington, J.L., 1952. A preliminary description of the Nigerian lead-zinc field. Econ. Geol. 47 (6), 583–608.
Fusswinkel, T., Wagner, T., Wenzel, T., Wälle, M., Lorenz, J., 2013. Evolution of unconformity-related MnFeAs vein mineralization, Sailauf (Germany): insight from major and trace elements in oxide and carbonate minerals. Ore Geol. Rev. 50, 28–51.
Fusswinkel, T., Wagner, T., Wenzel, T., Wälle, M., Lorenz, J., 2014. Red bed and basement sourced fluids recorded in hydrothermal mn–fe–as veins, Sailauf (Germany): a LA-ICPMS fluid inclusion study. Chem. Geol. 363, 22–39.
Göb, S., Loges, A., Nolde, N., Bau, M., Jacob, D.E., Markl, G., 2013. Major and trace element compositions (including REE) of mineral, thermal, mine and surface waters in SW Germany and implications for water–rock interaction. Appl. Geochem. 33, 127–152.
Grandia, F., Asmerom, Y., Getty, S., Cardellach, E., Canals, A., 2000. U–Pb dating of MVT ore-stage calcite: implications for fluid flow in a Mesozoic extensional basin from Iberian Peninsula. Journal of Geochemical Exploration 69, 377–380.
Haschke, S., Gutzmer, J., Wohlgemuth-Ueberwasser, C.C., Kraemer, D., Burisch, M., 2021. The Niederschlag fluorite-(baryte) deposit, Erzgebirge/Germany—A fluid inclusion and trace element study. Miner. Deposita 56, 1071–1086.
Henry, R.L., 2018. Low Temperature Aqueous Solubility of Fluorite at Temperatures of 5, 25, and 50° C and Ionic Strengths up to 0.72 M. Colorado School of Mines.
Hoeve, J., Sibbald, T.I., 1978. On the genesis of Rabbit Lake and other unconformity-type uranium deposits in northern Saskatchewan, Canada. Econ. Geol. 73 (8), 1450–1473.
Jungmann, M., Walter, B.F., Eiche, E., Giebel, R.J., Kolb, J., 2025. The source of lithium in connate fluids: evidence from the geothermal reservoir at Soultz-sous-Forêts, Upper Rhine Graben, France. J. Geochem. Explor. 270, 107641.
Keim, M.F., Walter, B.F., Neumann, U., Kreissl, S., Bayerl, R., Markl, G., 2019. Polyphase enrichment and redistribution processes in silver-rich mineral associations of the hydrothermal fluorite-baryte-(Ag-Cu) Clara deposit, SW Germany. Miner. Deposita 54, 155–174.
Kluge, T., Eiche, E., Walter, B., Kramar, U., Göttlicher, J., Gudelius, D., Giebel, J., Kolb, J., 2024. The influence of fluid pressure, redox potential and crystal growth characteristics in mississippi-valley-type (MVT) ore formation-lessons from a modern geothermal scale. Miner. Deposita 1–21.
Köhler, J., Schönenberger, J., Upton, B., Markl, G., 2009. Halogen and trace-element chemistry in the Gardar Province, South Greenland: subduction-related mantle metasomatism and fluid exsolution from alkalic melts. Lithos 113 (3–4), 731–747.

Kolchugin, A.N., Immenhauser, A., Walter, B.F., Morozov, V.P., 2016. Diagenesis of the palaeo-oil-water transition zone in a Lower Pennsylvanian carbonate reservoir: constraints from cathodoluminescence microscopy, microthermometry, and isotope geochemistry. Mar. Petrol. Geol. 72, 45–61.
Kolchugin, A., Immenhauser, A., Morozov, V., Walter, B., Eskin, A., Korolev, E., Neuser, R., 2020. A comparative study of two Mississippian dolostone reservoirs in the Volga-Ural Basin, Russia. J. Asian Earth Sci. 199, 104465.
Kreissl, S., Gerdes, A., Walter, B.F., Neumann, U., Wenzel, T., Markl, G., 2018. Reconstruction of a> 200 Ma multi-stage "five element" Bi-Co-Ni-Fe-As-S system in the Penninic Alps, Switzerland. Ore Geol. Rev. 95, 746–788.
Ladenburger, S., Walter, B.F., Marks, M.A., Markl, G., 2020. Combining ion chromatography and total reflection X-ray fluorescence for detection of major, minor and trace elements in quartz-hosted fluid inclusions. J. Anal. Chem. 75, 1477–1485.
Laier, T., Nielsen, B.L., 1989. Cementing halite in Triassic Bunter Sandstone (Tønder, southwest Denmark) as a result of hyperfiltration of brines. Chem. Geol. 76 (3–4), 353–363.
Leach, D.L., Marsh, E., Emsbo, P., Rombach, C.S., Kelley, K.D., Anthony, M., 2004. Nature of hydrothermal fluids at the shale-hosted red dog zn-pb-ag deposits, Brooks Range, Alaska. Econ. Geol. 99 (7), 1449–1480.
Malinverno, A., 2012. Evolution of the Tyrrhenian Sea-Calabrian Arc system: the past and the present. Rendiconti Online della Società Geologica Italiana 21 (1), 11–15.
Markl, G., Burisch, M., Neumann, U., 2016. Natural fracking and the genesis of five-element veins. Miner. Deposita 51, 703–712.
McCaig, A.M., Tritlla, J., Banks, D.A., 2000. Fluid mixing and recycling during pyrenean thrusting: evidence from fluid inclusion halogen ratios. Geochem. Cosmochim. Acta 64 (19), 3395–3412.
Mueller, Mathias, Igbokwe, Onyedika A., Walter, Benjamin, Pederson, Chelsea L., Riechelmann, Sylvia, Richter, Detlev K., Albert, Richard, et al., 2020. Testing the preservation potential of early diagenetic dolomites as geochemical archives. Sedimentology 67 (2), 849–881.
Nassar, N.T., Pineault, D., Allen, S.M., McCaffrey, D.M., Padilla, A.J., Brainard, J.L., Bayani, M., Shojaeddini, E., Ryter, J.W., Lincoln, S., Alonso, E., 2025. Methodology and technical input for the 2025 US List of Critical Minerals—Assessing the potential effects of mineral commodity supply chain disruptions on the US economy (No. 2025-1047). US Geological Survey.
Nordstrom, D.K., Jenne, E.A., 1977. Fluorite solubility equilibria in selected geothermal waters. Geochem. Cosmochim. Acta 41 (2), 175–188.
Obaje, N.G., 2009. Geology and Mineral Resources of Nigeria, 120. Springer, Berlin, p. 221.
Obaje, N.G., Wehner, H., Abubakar, M.B., Isah, M.T., 2004. Nasara-I well, Gongola Basin (Upper Benue Trough, Nigeria): source-rock evaluation. J. Petrol. Geol. 27 (2), 191–206.
Obiora, D.N., Ossai, M.N., Okeke, F.N., Oha, A.I., 2016. Interpretation of airborne geophysical data of Nsukka area, Southeastern Nigeria. J. Geol. Soc. India 88, 654–667.
Oden, M.I., 2012. Baryte veins in the Benue Trough: field characteristics, the quality issue and some tectonic implications. Environ. Nat. Resour. Res. 2 (2), 21.
Offodile, M.E., 1975. A review of the geology of the Benue Trough, Nigeria. J. Afr. Earth Sci. 3, 283–291.
Offodile, M.E., 1976. The Geology of the Middle Benue, 4. Palaentological Institute, University Uppsala, Special Publication, Nigeria, pp. 1–166.
Ofoegbu, C.O., Odigi, M.I., 1989. Basement structures and ore mineralization in the Benue Trough. the Benue Trough: structure and Evolution. In: Ofoegbu, C.O. (Ed.), Earth Evol, Sci, pp. 239–248.
Ogg, J.G., 2012. Triassic. The Geologic Time Scale, pp. 681–730.
Olade, M.A., Morton, R.D., 1985. Origin of lead-zinc mineralization in the southern Benue Trough, Nigeria—Fluid inclusion and trace element studies. Miner. Deposita 20, 76–80.
Omada, J., 1985. The Geology and Geochemistry of Baryte Mineralization in the Azara area, Middle Benue Trough, Nigeria Doctoral Dissertation, 243pp.
Omada, J.I., Ike, E.C., 1996. On the economic appraisal and genesis of the baryte mineralisation and saline springs in the middle Benue trough, Nigeria. Journal of Mineralogy, Petrology and Economic Geology 91 (3), 109–115.
Petters, S.W., Ekweozor, C.M., 1982. Petroleum geology of Benue trough and southeastern Chad basin, Nigeria. AAPG (Am. Assoc. Pet. Geol.) Bull. 66 (8), 1141–1149.
Rddad, L., Cherai, M., Walter, B.F., Talbi, F., 2025. Multistage ore-forming processes in the genesis of the fluorite-baryte Merguechoum ore deposit (Moroccan eastern Meseta) in relation to Pangaea rifting. J. Geochem. Explor. 275, 107766.
Rddad, L., Cherai, M., Walter, B.F., Talbi, F., Kraemer, D., Billström, K., 2024a. Geochemistry and fluid inclusion study of the Jbel Tirremi fluorite-baryte deposit, Morocco: new insights into the genetic model in relation to Mesozoic tectonics. Geochemistry 84 (3), 126162.
Rddad, L., Jemmali, N., Jaballah, S., 2024b. The role of organic matter and hydrocarbons in the genesis of the pb-zn-fe (Ba-Sr) ore deposits in the diapirs Zone, Northern Tunisia. Minerals 14 (9), 932.
Rddad, L., Sośnicka, M., Abdelhafid, E., Kraemer, D., Billström, K., Mourad, E., Toummite, A., 2023. Fluid evolution and origin of the Tamazert fluorite deposits, Moroccan High Atlas. J. Afr. Earth Sci. 200, 104856.
Rddad, L., Kraemer, D., Walter, B.F., Darling, R., Cousens, B., 2022. Unravelling the fluid flow evolution and precipitation mechanisms recorded in calcite veins in relation to Pangaea rifting–Newark Basin, USA. Geochemistry 82 (4), 125918.
Richard, A., Cathelineau, M., Boiron, M.C., Mercadier, J., Banks, D.A., Cuney, M., 2016. Metal-rich fluid inclusions provide new insights into unconformity-related U deposits (Athabasca Basin and Basement, Canada). Miner. Deposita 51 (2), 249–270.
Reyment, R.A., 1965. Aspects of the Geology of Nigeria: the Stratigraphy of the Cretaceous and Cenozoic Deposits *(No Title)*.
Scharrer, M., Epp, T., Walter, B., Pfaff, K., Vennemann, T., Markl, G., 2022. The formation of (Ni-Co-Sb)-Ag-As ore shoots in hydrothermal galena-sphalerite-fluorite veins. Mineralium Deposita 57 (5), 853–885.
Scharrer, M., Fusswinkel, T., Markl, G., 2023. Triple-halogen (Cl-Br-I) fluid inclusion LA-ICP-MS microanalysis to unravel iodine behavior and sources during marine fluid infiltration into the basement in unconformity settings. Geochem. Cosmochim. Acta 357, 64–76.
Scharrer, M., Kreissl, S., Markl, G., 2019. The mineralogical variability of hydrothermal native element-arsenide (five-element) associations and the role of physicochemical and kinetic factors concerning sulfur and arsenic. Ore Geol. Rev. 113, 103025.
Scharrer, M., Reich, R., Fusswinkel, T., Walter, B.F., Markl, G., 2021. Basement aquifer evolution and the formation of unconformity-related hydrothermal vein deposits: LA-ICP-MS analyses of single fluid inclusions in fluorite from SW Germany. Chem. Geol. 575, 120260.
Seo, J.H., Guillong, M., Aerts, M., Zajacz, Z., Heinrich, C.A., 2011. Microanalysis of S, Cl, and Br in fluid inclusions by LA–ICP-MS. Chem. Geol. 284 (1–2), 35–44.
Staude, S., Bons, P.D., Markl, G., 2009. Hydrothermal vein formation by extension-driven dewatering of the middle crust: an example from SW Germany. Earth Planet Sci. Lett. 286 (3–4), 387–395.
Steele-MacInnis, M., Han, L., Lowell, R., Rimstidt, J., Bodnar, R., 2012. Quartz precipitation and fluid inclusion characteristics in sub-seafloor hydrothermal systems associated with volcanogenic massive sulfide deposits. Open Geosci. 4 (2), 275–286.
Stober, I., Bucher, K., 2004. Fluid sinks within the earth's crust. Geofluids 4 (2), 143–151.
Stober, I., Bucher, K., 2012. Hydraulic conductivity of fractured upper crust: insights from hydraulic tests in boreholes and fluid–rock interaction in crystalline basement rocks. Crustal Permeability 174–188.
Subías, I., Fernández-Nieto, C., 1995. Hydrothermal events in the Valle de Tena (Spanish Western Pyrenees) as evidenced by fluid inclusions and trace-element distribution from fluorite deposits. Chem. Geol. 124 (3–4), 267–282.
Tijani, M.N., 2004. Evolution of saline waters and brines in the Benue-Trough, Nigeria. Appl. Geochem. 19 (9), 1355–1365.
Tijani, M.N., Loehnert, E.P., Uma, K.O., 1996. Origin of saline groundwaters in the Ogoja area, Lower Benue Trough, Nigeria. J. Afr. Earth Sci. 23 (2), 237–252.
Uma, K.O., Loehnert, E.P., 1994. Hydraulic conductivity of shallow sandy aquifers: effects of sedimentologic and diagenetic differences. Environ. Geol. 23, 171–181.
Walter, B.F., Gerdes, A., Kleinhanns, I.C., Dunkl, I., von Eynatten, H., Kreissl, S., Markl, G., 2018a. The connection between hydrothermal fluids, mineralization, tectonics and magmatism in a continental rift setting: Fluorite Sm-Nd and hematite and carbonates U-Pb geochronology from the Rhinegraben in SW Germany. Geochimica et Cosmochimica Acta 240, 11–42.
Walter, B.F., Giebel, R.J., Arthuzzi, J.C., Kemmler, L., Kolb, J., 2024. Diatreme-hosted fluorite mineralization in S-Namibia–A tale of cryogenic brine formation and fluid mixing below an unconformity in the context of pangea rifting. J. Afr. Earth Sci. 210, 105154.
Walter, B.F., Burisch, M., Fusswinkel, T., Marks, M.A., Steele-MacInnis, M., Wälle, M., Apukhtina, O., Markl, G., 2018b. Multi-reservoir fluid mixing processes in rift-related hydrothermal veins, Schwarzwald, SW-Germany. Journal of Geochemical Exploration 186, 158–186.
Walter, B.F., Burisch, M., Markl, G., 2016. Long-term chemical evolution and modification of continental basement brines–a field study from the Schwarzwald, SW Germany. Geofluids 16 (3), 604–623.
Walter, B.F., Burisch, M., Marks, M.A., Markl, G., 2017. Major element compositions of fluid inclusions from hydrothermal vein-type deposits record eroded sedimentary units in the Schwarzwald district, SW Germany. Miner. Deposita 52, 1191–1204.
Walter, B.F., Giebel, R.J., Arthuzzi, J.C., Kemmler, L., Kolb, J., 2024. Diatreme-hosted fluorite mineralization in S-Namibia–A tale of cryogenic brine formation and fluid mixing below an unconformity in the context of Pangea rifting. Journal of African Earth Sciences 210, 105154.
Walter, B.F., Giebel, R.J., Siegfried, P., Doggart, S., Macey, P., Schiebel, D., Kolb, J., 2023. The genesis of hydrothermal veins in the Aukam valley SW Namibia–A far field consequence of Pangean rifting? Journal of Geochemical Exploration 250, 107229.
Walter, B.F., Immenhauser, A., Geske, A., Markl, G., 2015. Exploration of hydrothermal carbonate magnesium isotope signatures as tracers for continental fluid aquifers, Schwarzwald mining district, SW Germany. Chemical Geology 400, 87–105.
Walter, B.F., Kortenbruck, P., Scharrer, M., Zeitvogel, C., Wälle, M., Mertz-Kraus, R., Markl, G., 2019. Chemical evolution of ore-forming brines–Basement leaching, metal provenance, and the redox link between barren and ore-bearing hydrothermal veins. A case study from the Schwarzwald mining district in SW-Germany. Chem. Geol. 506, 126–148.
Wilkinson, J.J., 2010. A review of fluid inclusion constraints on mineralization in the Irish ore field and implications for the genesis of sediment-hosted Zn-Pb deposits. Econ. Geol. 105 (2), 417–442.
Yenne, E., Green, C., Torvela, T., 2025. Modelling geologic features and structures in the Middle and Lower Benue Trough of Nigeria from gravity and aeromagnetic data sets. J. Afr. Earth Sci. 231, 105745.